symmetry

MDPI

Article

Self-Similarity of Continuous-Spectrum Radiative Transfer in Plasmas with Highly Reflecting Walls

Alexander B. Kukushkin [1,2,3]* and Pavel V. Minashin [1]

[1] National Research Center "Kurchatov Institute", 123182 Moscow, Russia;
[2] National Research Nuclear University MEPhI Moscow Engineering Physics Institute, 115409 Moscow, Russia;
[3] Moscow Institute of Physics and Technology, National Research University, 141700 Dolgoprudny, Moscow Region, Russia;
* Correspondence: Kukushkin_AB@nrcki.ru;

Abstract: Radiative Transfer (RT) in continuous spectrum in plasmas is caused by the emission and absorption of electromagnetic waves (EM) by free electrons. For a wide class of problems, the deviation of the velocity distribution function (VDF) of free electrons from the thermodynamic equilibrium, the Maxwellian VDF, can be neglected. In this case, RT in the geometric optics approximation is reduced to a single transport equation for the intensity of EM waves with source and sink functions dependent on the macroscopic parameters of the plasma (temperature and density of electrons). Integration of this equation for RT of radio-frequency EM waves in laboratory plasmas with highly reflecting metallic walls is substantially complicated by the multiple reflections which make the waves with the long free path the dominant contributors to the power balance profile. This in turn makes the RT substantially nonlocal with the spatial-spectral profile of the power balance determined by the spatial integrals of the plasma parameters. The geometric symmetry of the bounding walls, especially when enhanced by the diffuse reflectivity, provides a semi-analytic description of the RT problem. Analysis of the accuracy of such an approach reveals an approximate self-similarity of the power balance profile and the radiation intensity spectrum in both approximate and *ab initio* modeling. This phenomenon is shown here for a wide range of plasma parameters and wall reflectivity, including data from various numeric codes. The relationship between the revealed self-similarity and the accuracy of numeric codes is discussed.

Keywords: radiative transfer, continuous spectra, electron-cyclotron radiation; thermonuclear fusion plasma, tokamak-reactor; ITER

Citation: Lastname, F.; Lastname, F.; Lastname, F. Title. *Symmetry* **2021**, *13*, 1303. https://doi.org/10.3390/sym13071303

Academic Editor: Fabio Sattin

Received: 20 May 2021
Accepted: 7 July 2021
Published: 20 July 2021

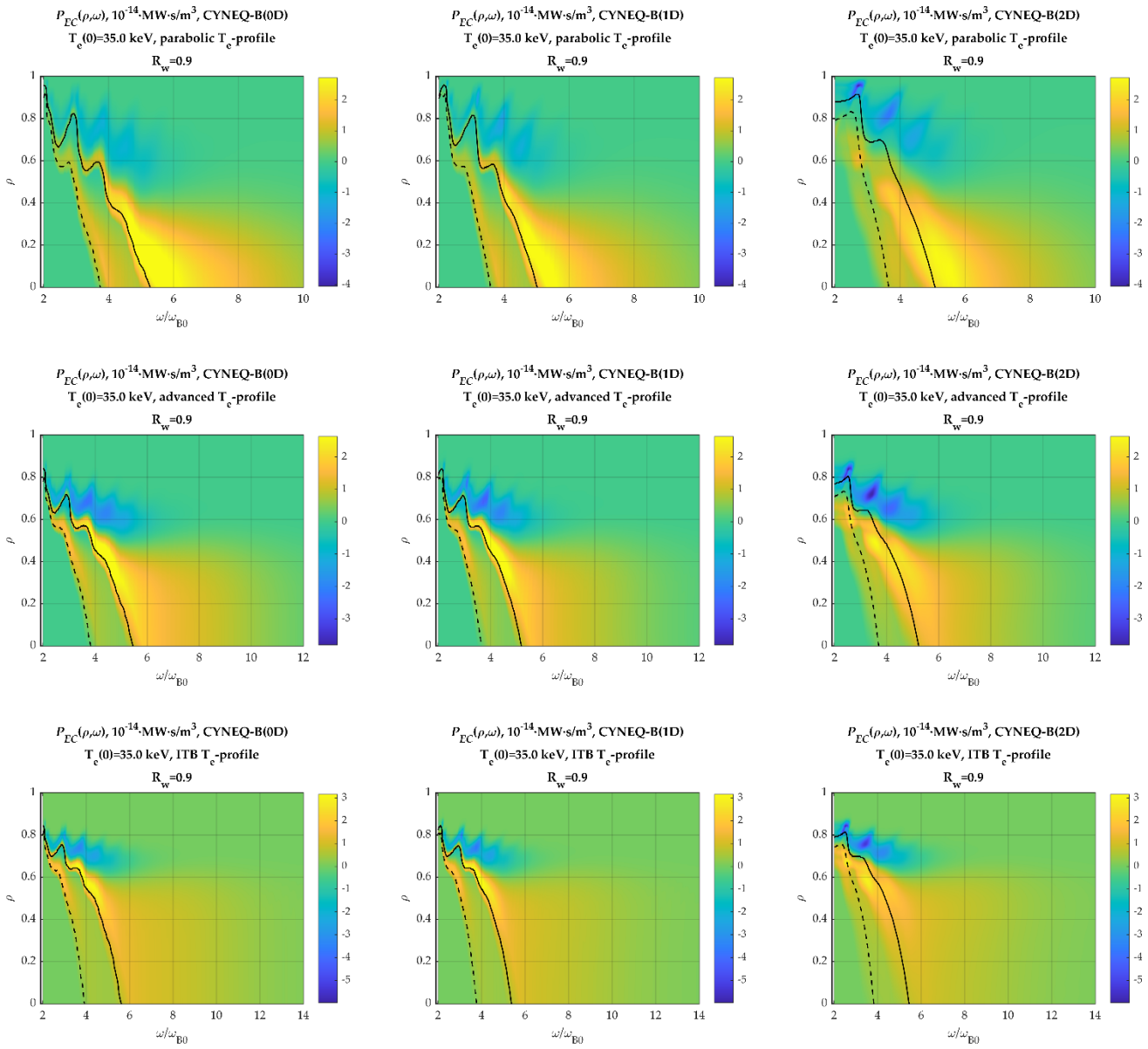

Figure S1. Spectral-spatial distribution of the EC power loss, calculated using CYNEQ code with different approximation of the magnetic field profile, for ITER-like scenario and different profiles of electron temperature with fixed central temperature T_e=35 keV (see Table 1), wall reflection coefficient R_w = 0.9. Boundaries between optically thick inner plasma and optically thin outer plasma are shown for two polarizations of the EC waves in plasma: X-mode (solid line) and O-mode (dashed line).

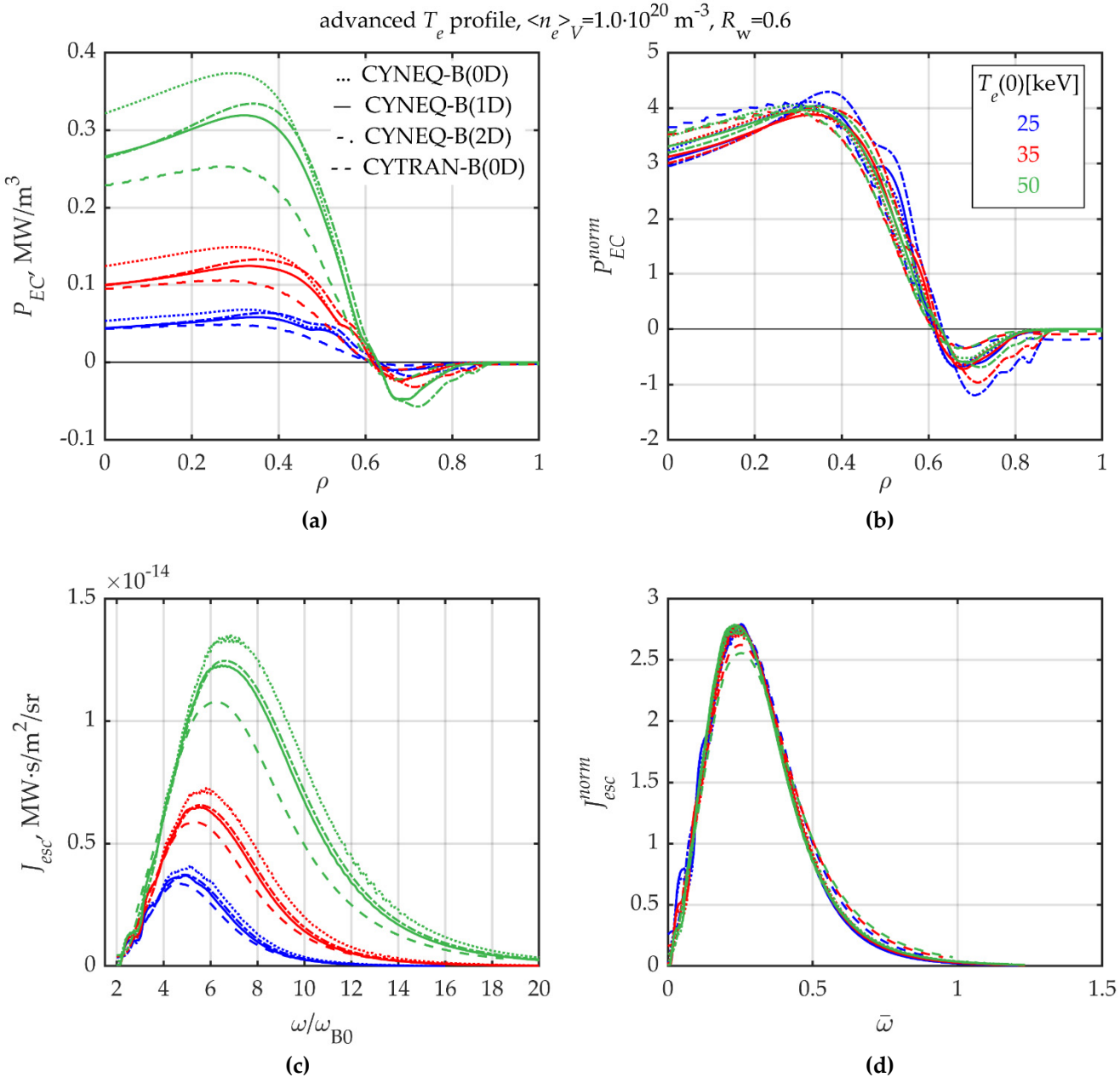

Figure S2. Self-similarity of ECR transport, calculated using the CYNEQ and CYTRAN codes, for tokamak-reactor conditions with a advanced profile of electron temperature, different values of the central temperature indicated in the inset, and a flat profile of the electron density (see Tables 1, 2 and (27)): **(a)** radial profile of the net EC power loss density (4) (the color of the curve corresponds to the central temperature indicated in the inset); **(b)** the corresponding normalized profiles of the net EC power loss density (20); **(c)** the spectral intensity of the escaping ECR (18); **(d)** the corresponding normalized spectra (25). The wall reflection coefficient is R_w=0.6. Plasma equilibrium was calculated using the ASTRA code, where for central temperatures $T_e(0)$ = 25 keV and 35 keV the plasma current was taken I_p = 15 MA, and for $T_e(0)$ = 50 keV, I_p = 20 MA.

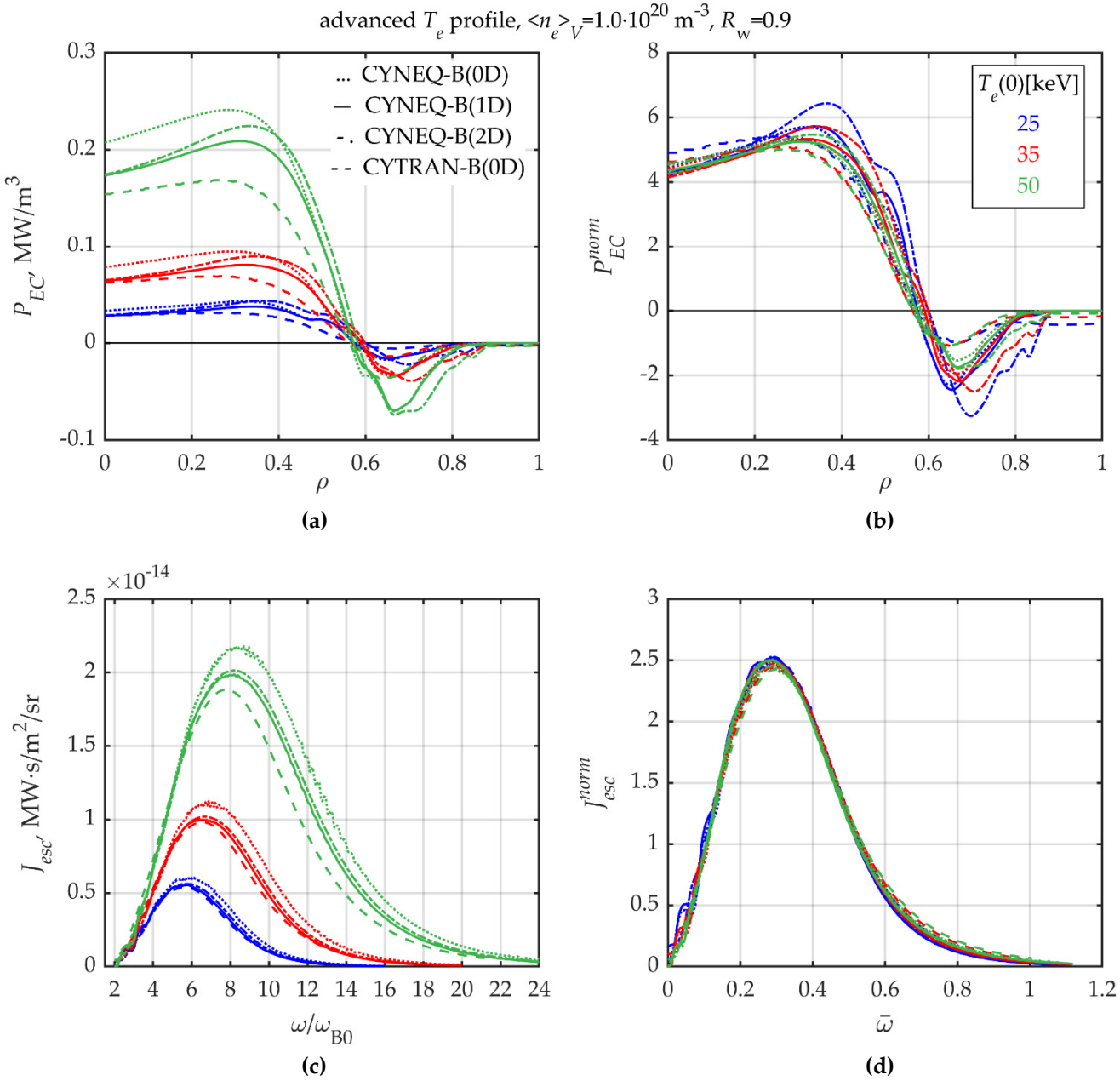

Figure S3. The same as in Figure S2 but for R_w=0.9 (see Table 1 and (27)).

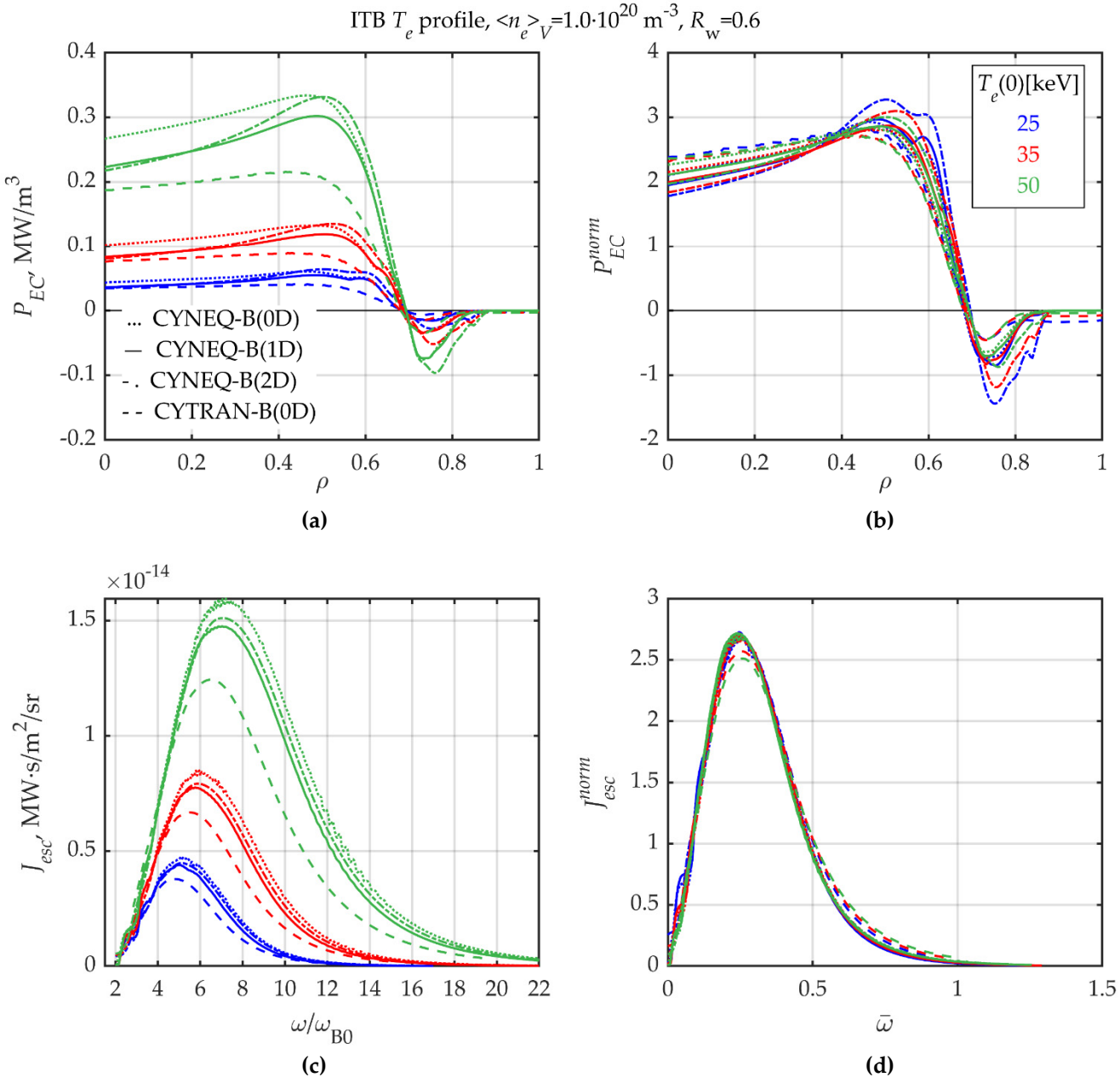

Figure S4. The same as in Figure S2 but for the ITB electron temperature profile (see Table 1 and (27)).

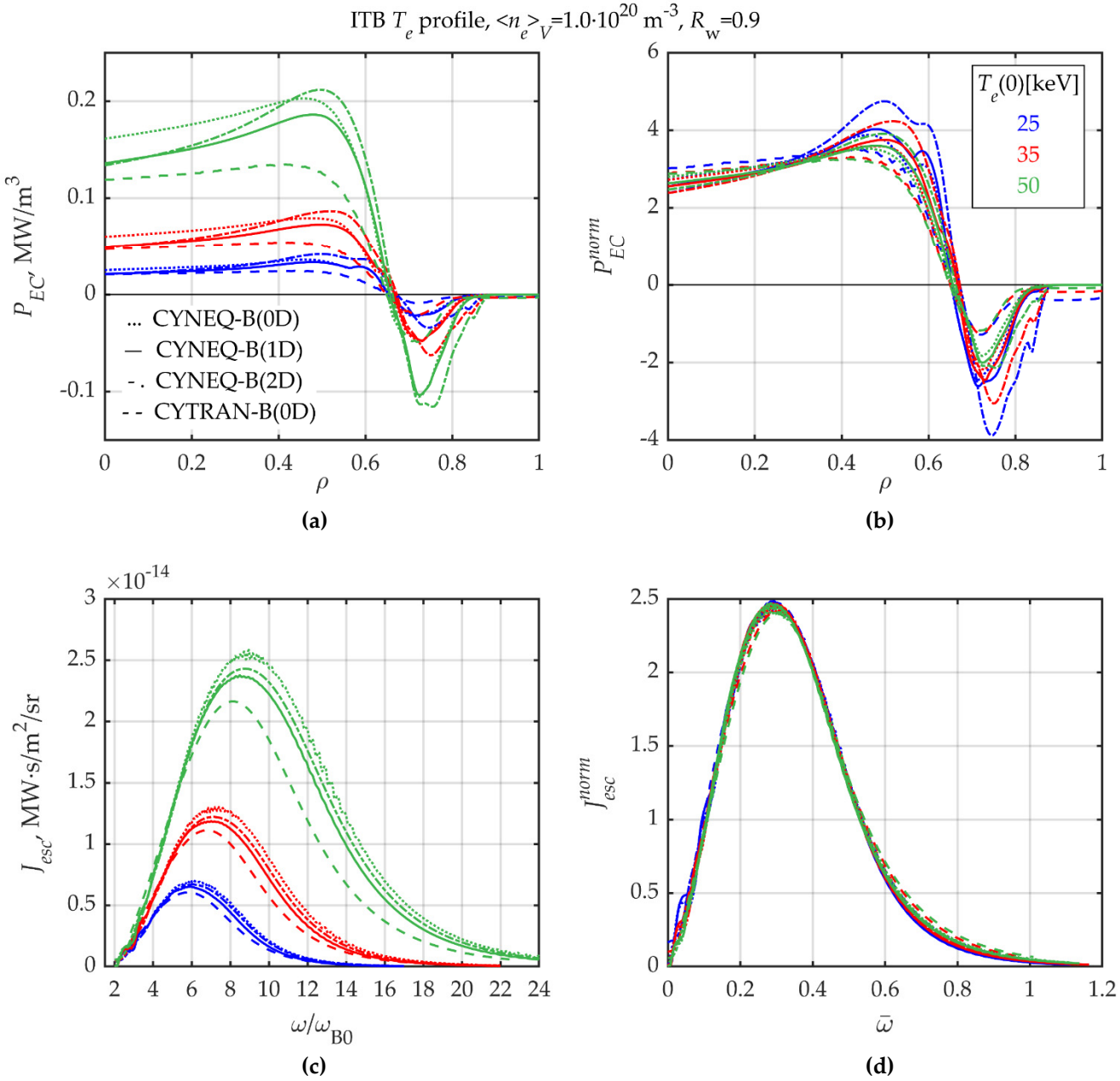

Figure S5. The same as in Figure S2 but for the ITB electron temperature profile and R_w=0.9 (see Table 1 and (27)).

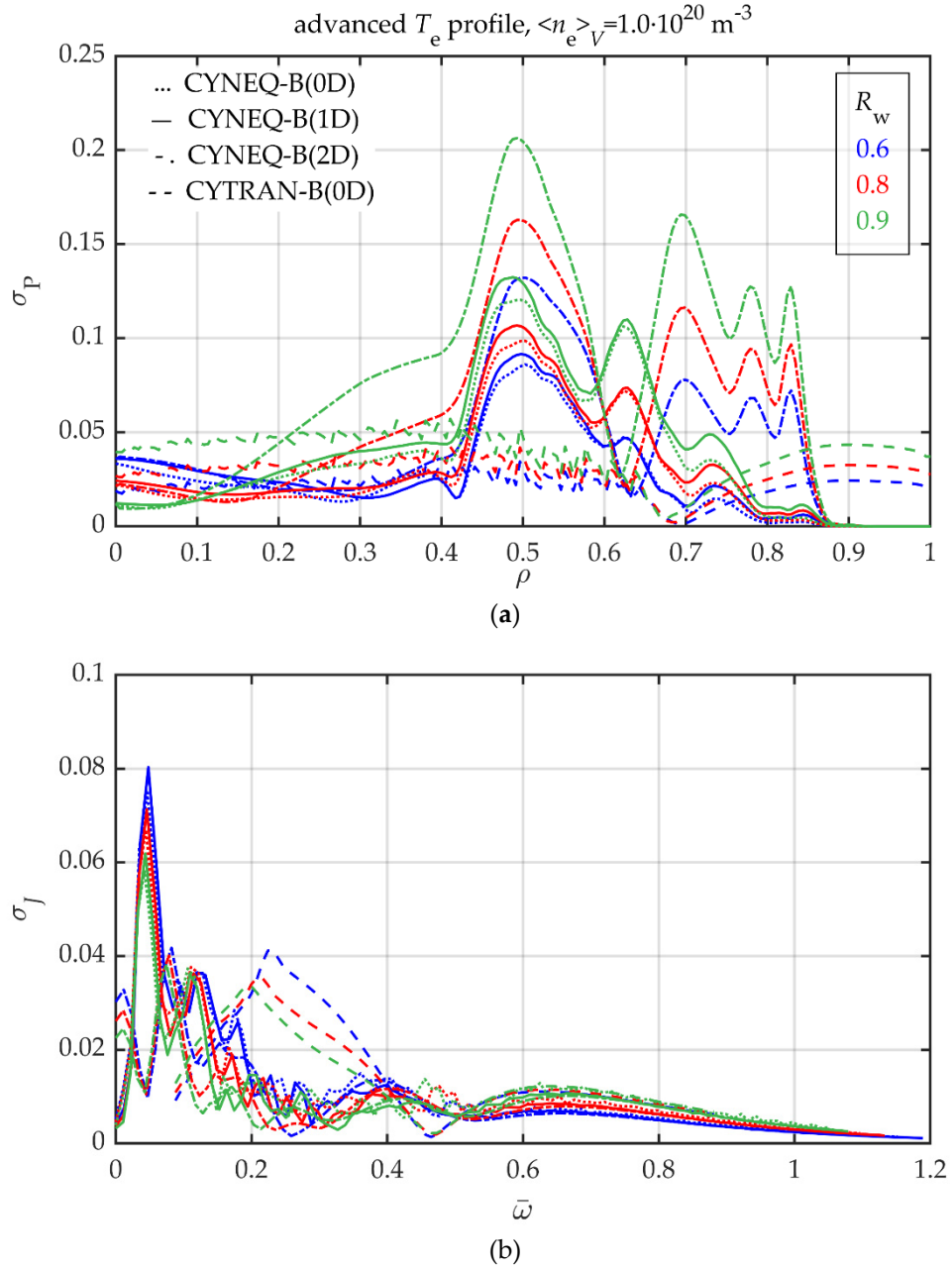

Figure S6. (**a**) Profiles of the relative deviation (30) of the normalized profiles of the EC power loss density from the mean normalized profile (28). (**b**) Profiles of the relative deviation (32) of the normalized spectral intensity of the escaping ECR from the mean normalized spectrum (29) for the advanced profile of T_e and the flat profile of n_e (see Table 1) and different values of R_w. The color of the curve corresponds to the R_w value in the inset.

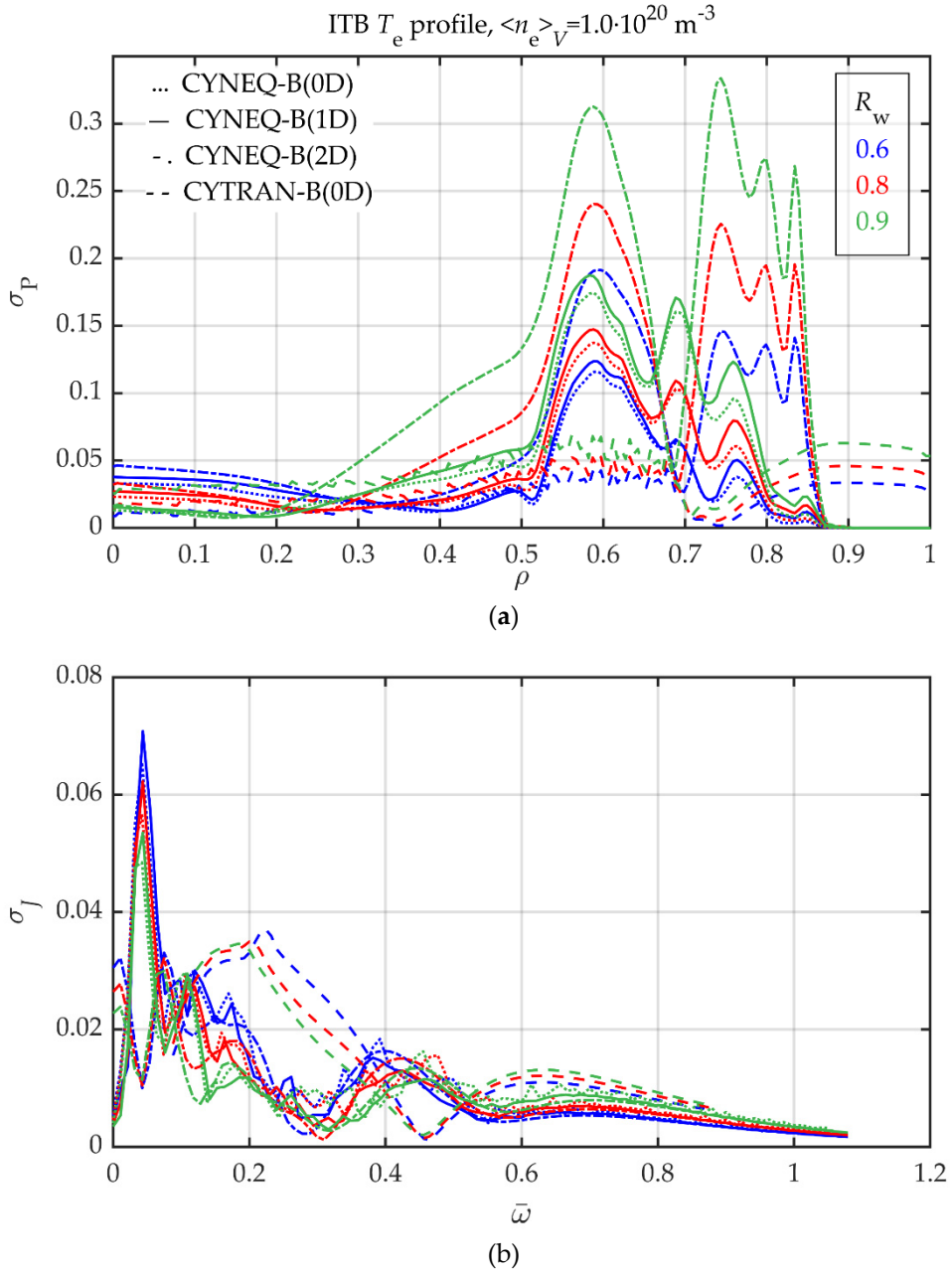

Figure S7. The same as in Figure S16 but for ITB temperature profile (see Table 1 and (27)).

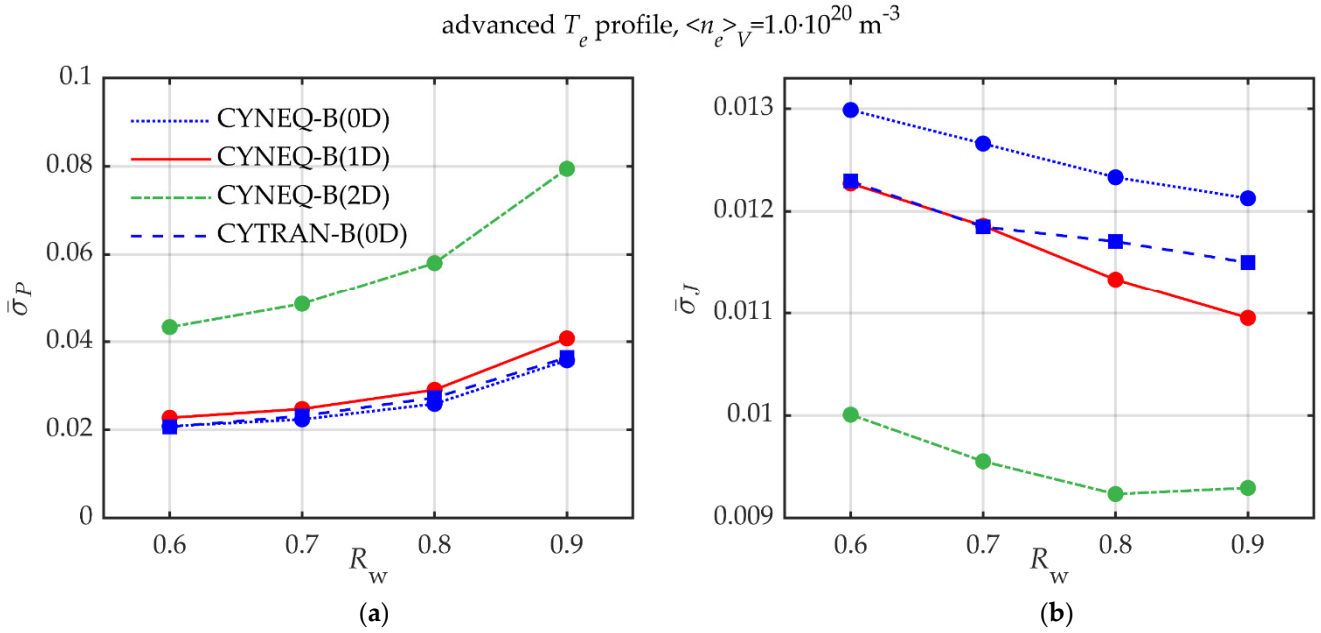

Figure S8. Volume-averaged deviation (31) of the normalized profile of the net EC power loss density from the mean normalized profile (28) (**a**), and spectrum-averaged deviation (33) of the normalized spectra of EC radiation intensity from the mean normalized spectrum (29) (**b**) as a function of the wall reflection coefficient for the advanced profile of the electron temperature and the flat profile of electron density (see Table 1 and (27)).

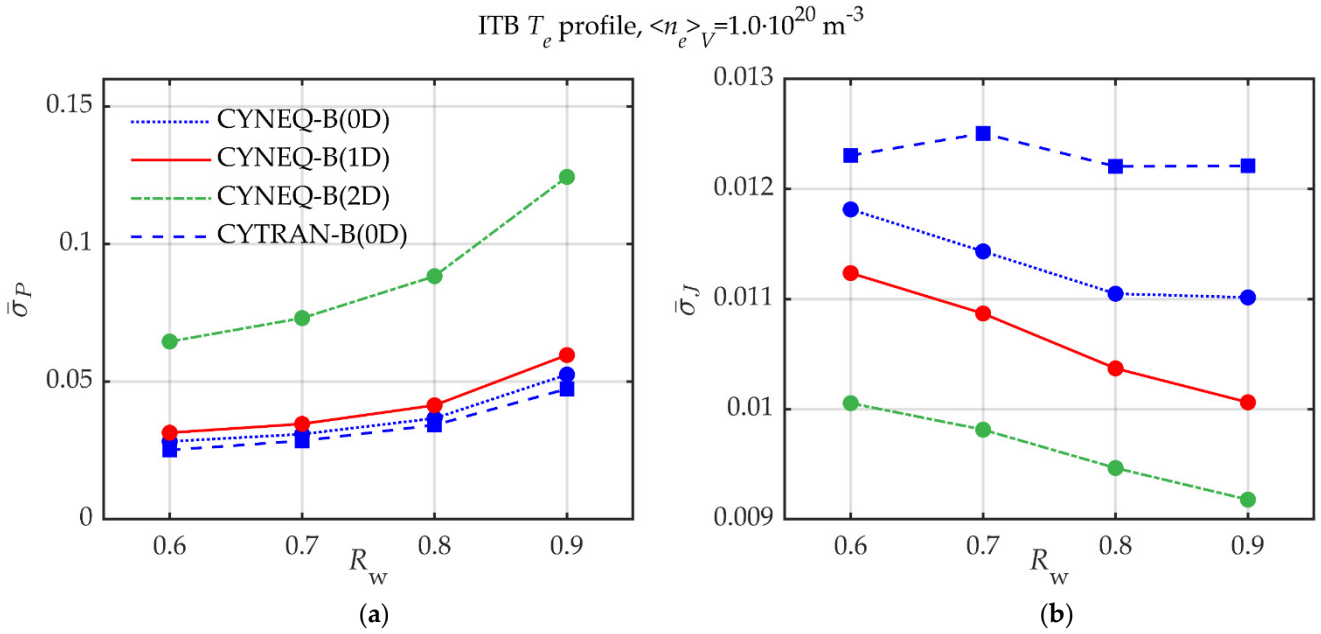

Figure S9. The same as in Figure S8 but for ITB temperature profile (see Table 1 and (27)).

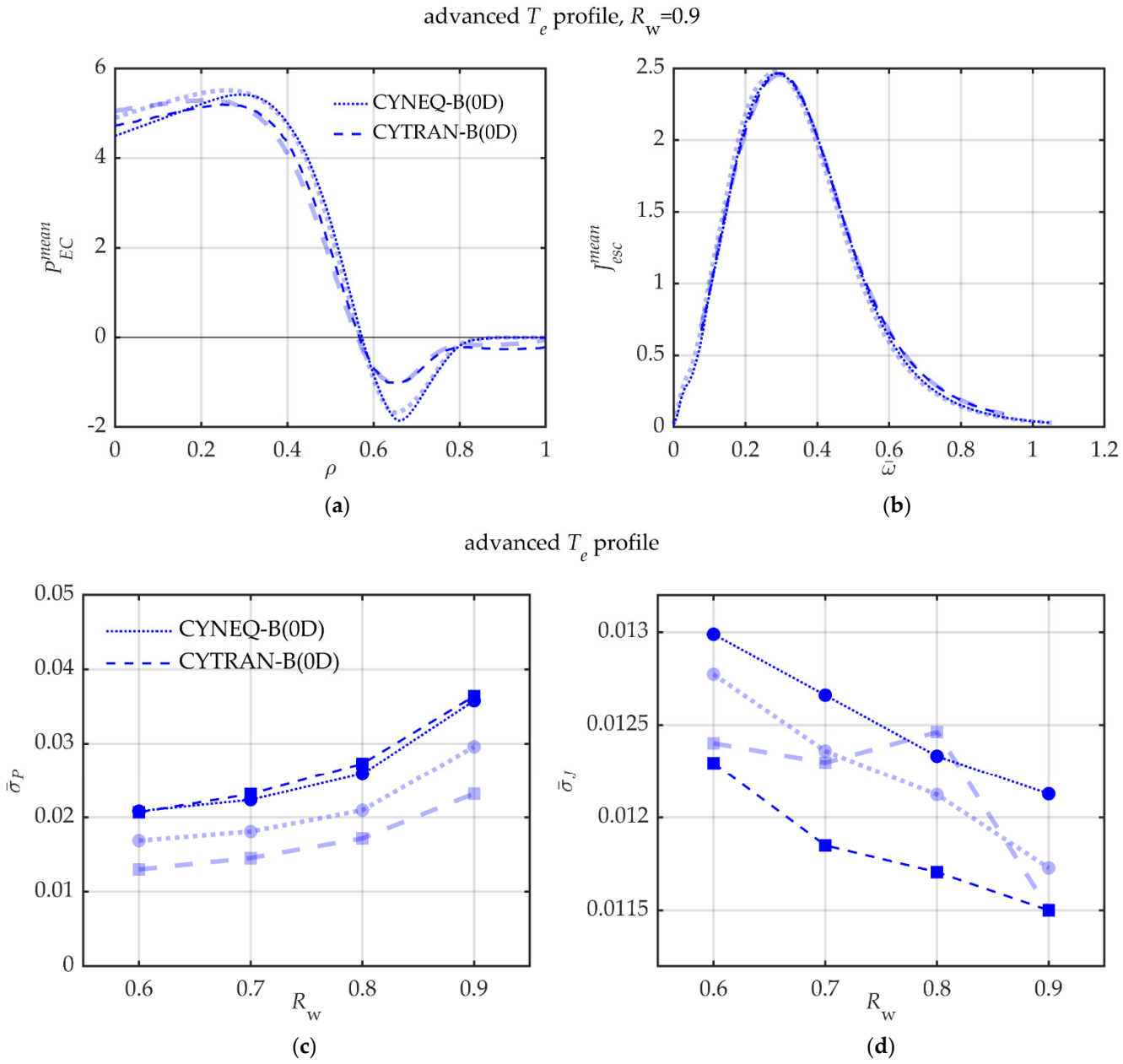

Figure S10. Comparison of the accuracy of the self-similarity for the flat (non-transparent thin lines) and non-flat (transparent thick lines) electron density profile, advanced temperature profile with different central temperatures in the range 20-55 keV (see Tables 1, 2 and (27)). (**a**) Mean profiles (28) of the normalized radial distribution of the net EC power loss density; (**b**) mean spectra (25) of the normalized intensity of EC radiation; (**c**) deviation (30) of the normalized profile of the net EC power loss density from the mean normalized profile; (**d**) deviation (32) of the normalized spectra of EC radiation intensity from the mean spectrum.

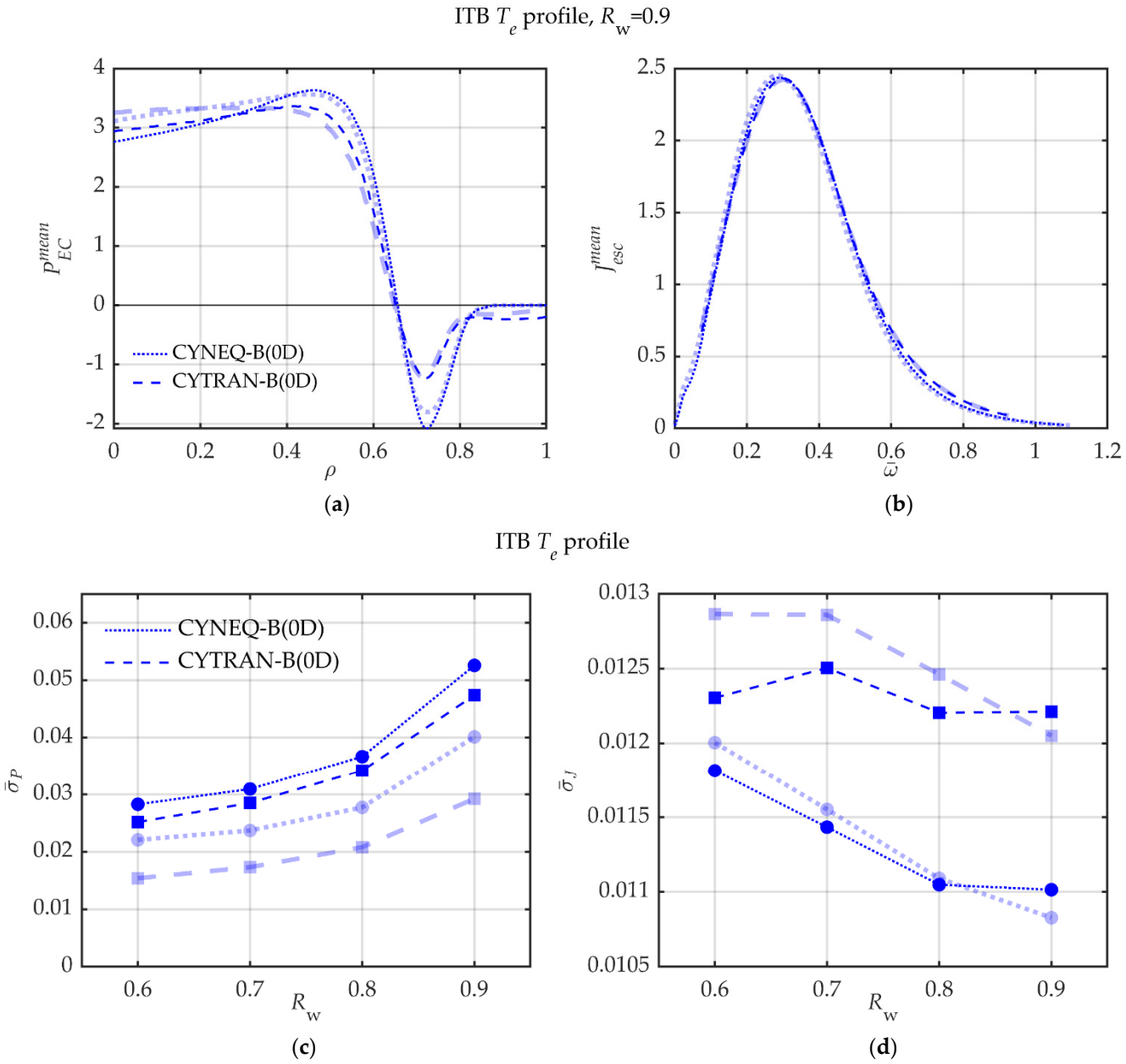

Figure S11. The same as in Figure S10 but for ITB temperature profile (see Tables 1, 2 and (27)).

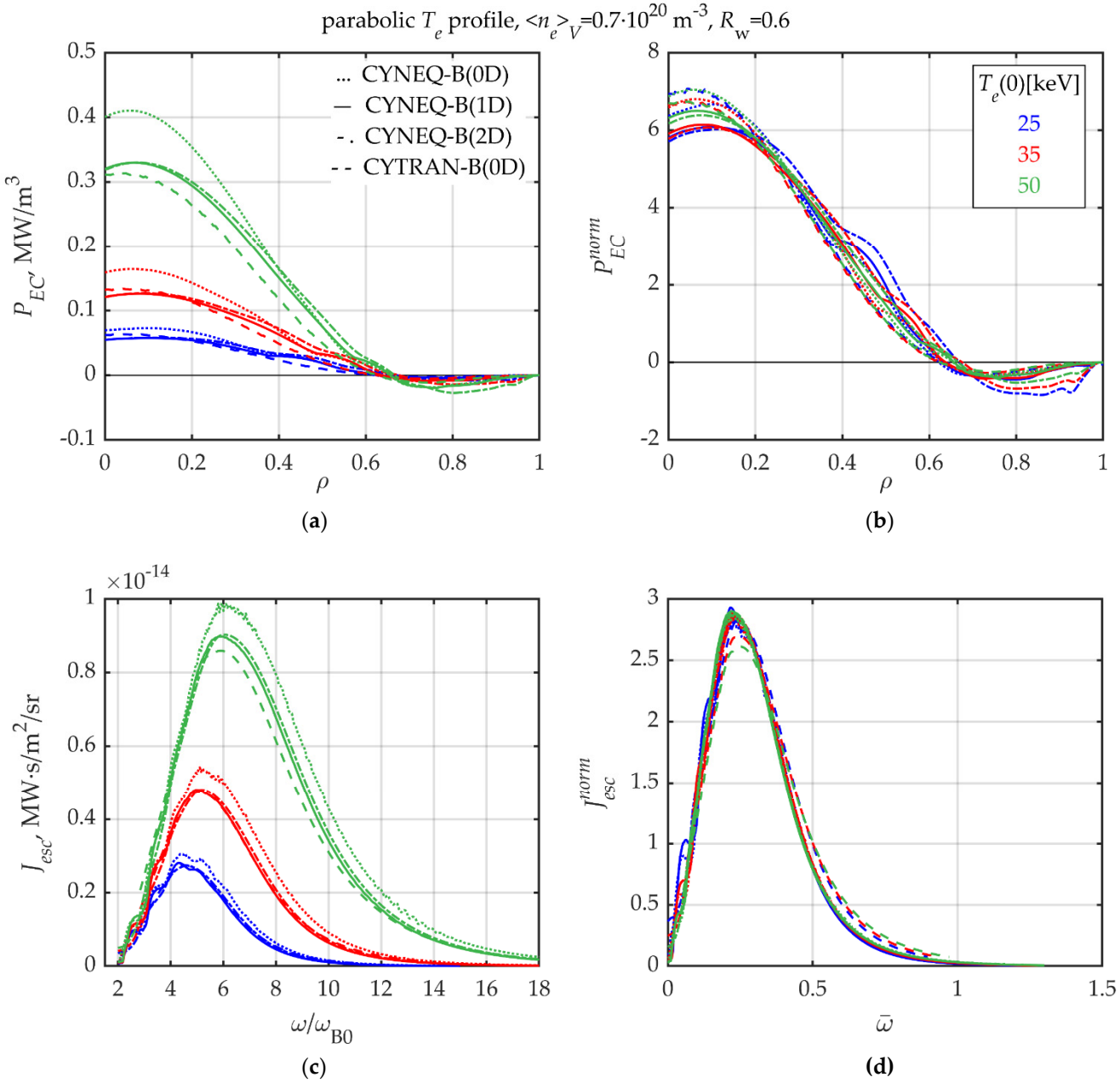

Figure S12. Self-similarity of ECR transport, calculated using the CYNEQ and CYTRAN codes, for tokamak-reactor conditions with a parabolic profile of electron temperature, different values of the central temperature indicated in the inset, and a non-flat profile of the electron density (see Tables 1,2 and eq. (27)): **(a)** radial profile of the net EC power loss density (4) (the color of the curve corresponds to the central temperature indicated in the inset); **(b)** the corresponding normalized profiles of the net EC power loss density (20); **(c)** the spectral intensity of the escaping ECR (19); **(d)** the corresponding normalized spectra (25). The wall reflection coefficient is R_w=0.6. Plasma equilibrium was calculated using the ASTRA code, where for central temperatures $T_e(0)$ = 25 keV and 35 keV the plasma current was taken I_p = 15 MA, and for $T_e(0)$ = 50 keV, I_p = 20 MA.

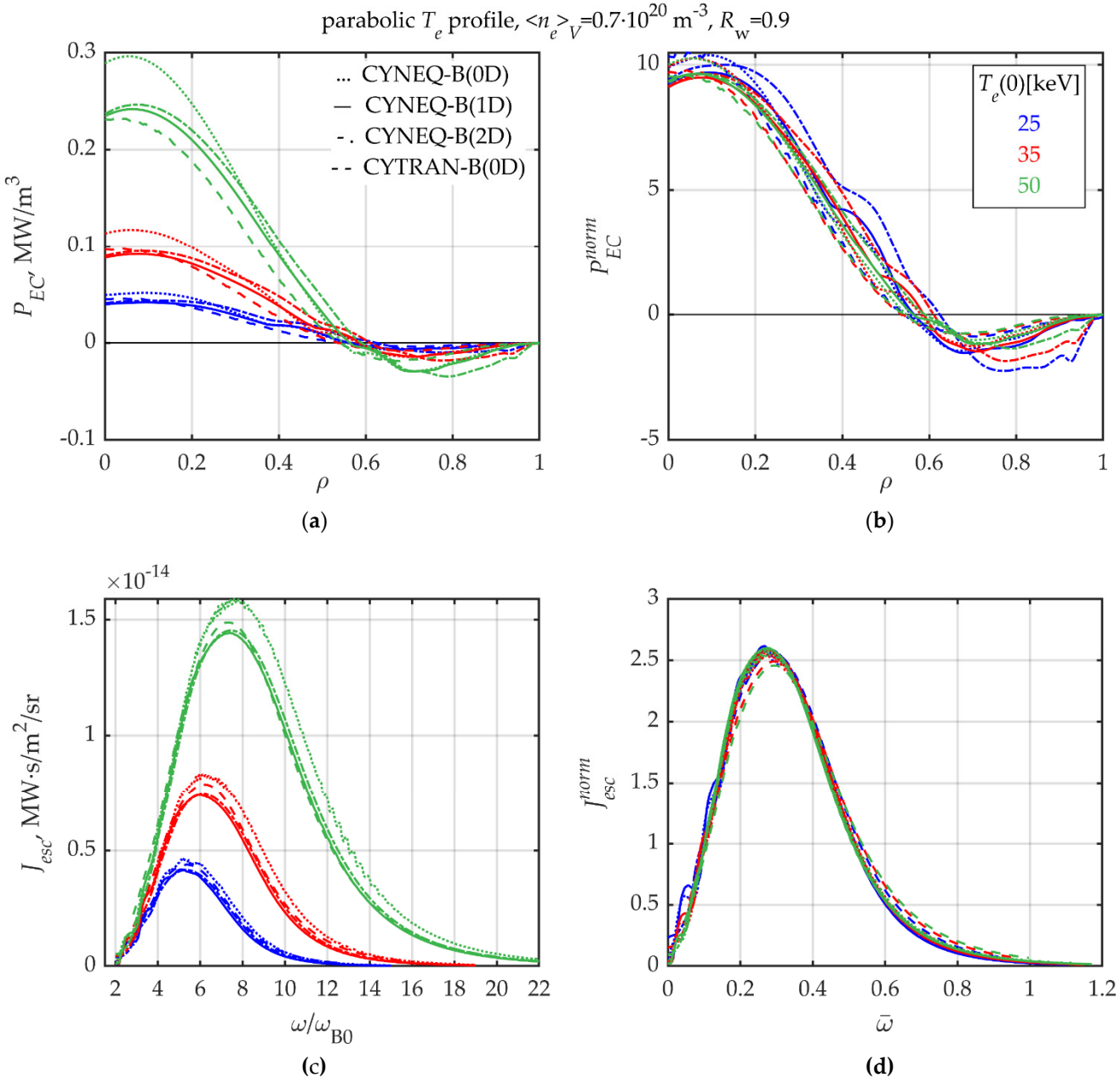

Figure S13. The same as in Figure S12 but for the wall reflection coefficient R_w = 0.9.

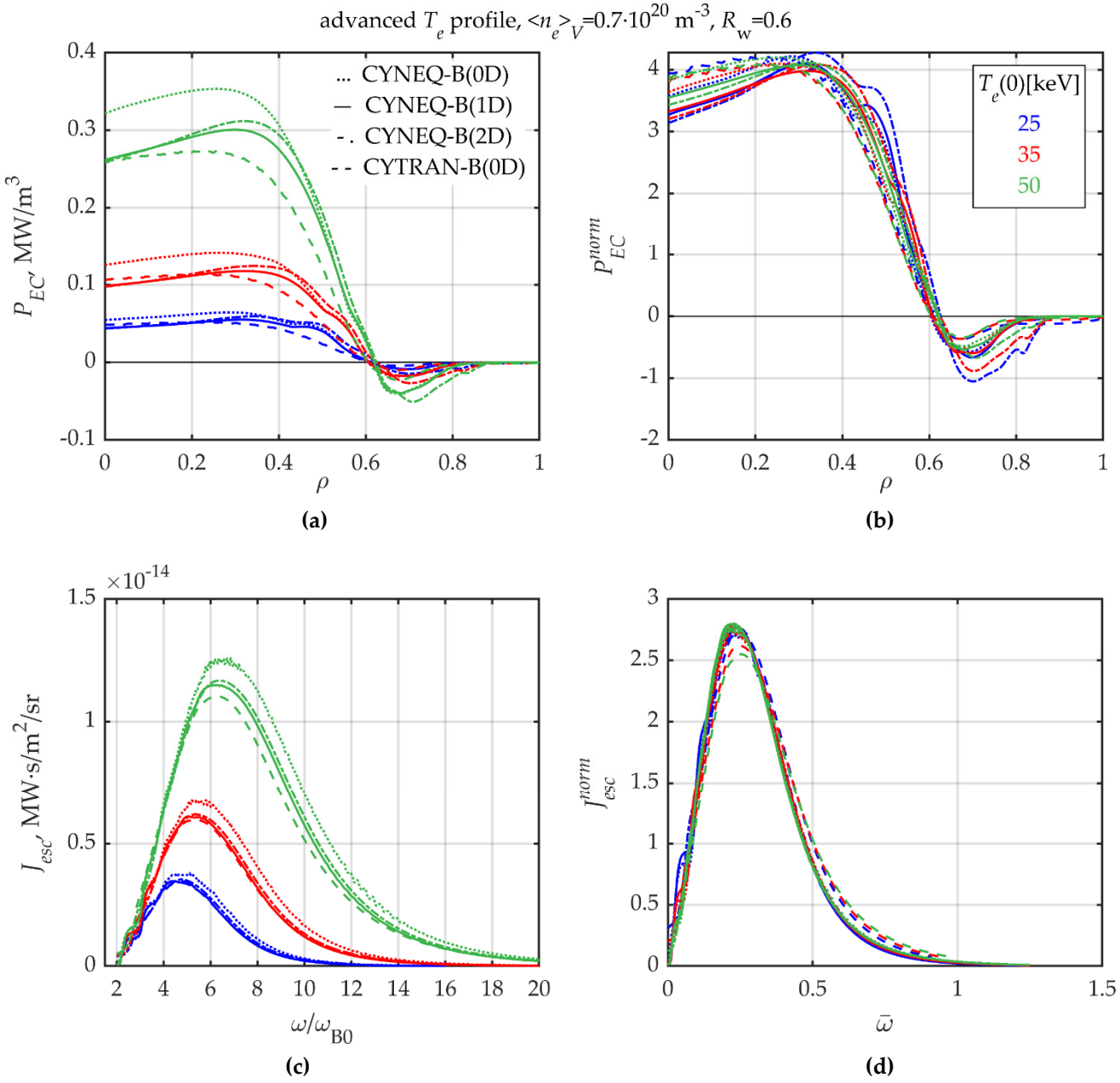

Figure S14. The same as in Figure S12 but for the advanced electron temperature profile (see Table 1 and eq. (27)).

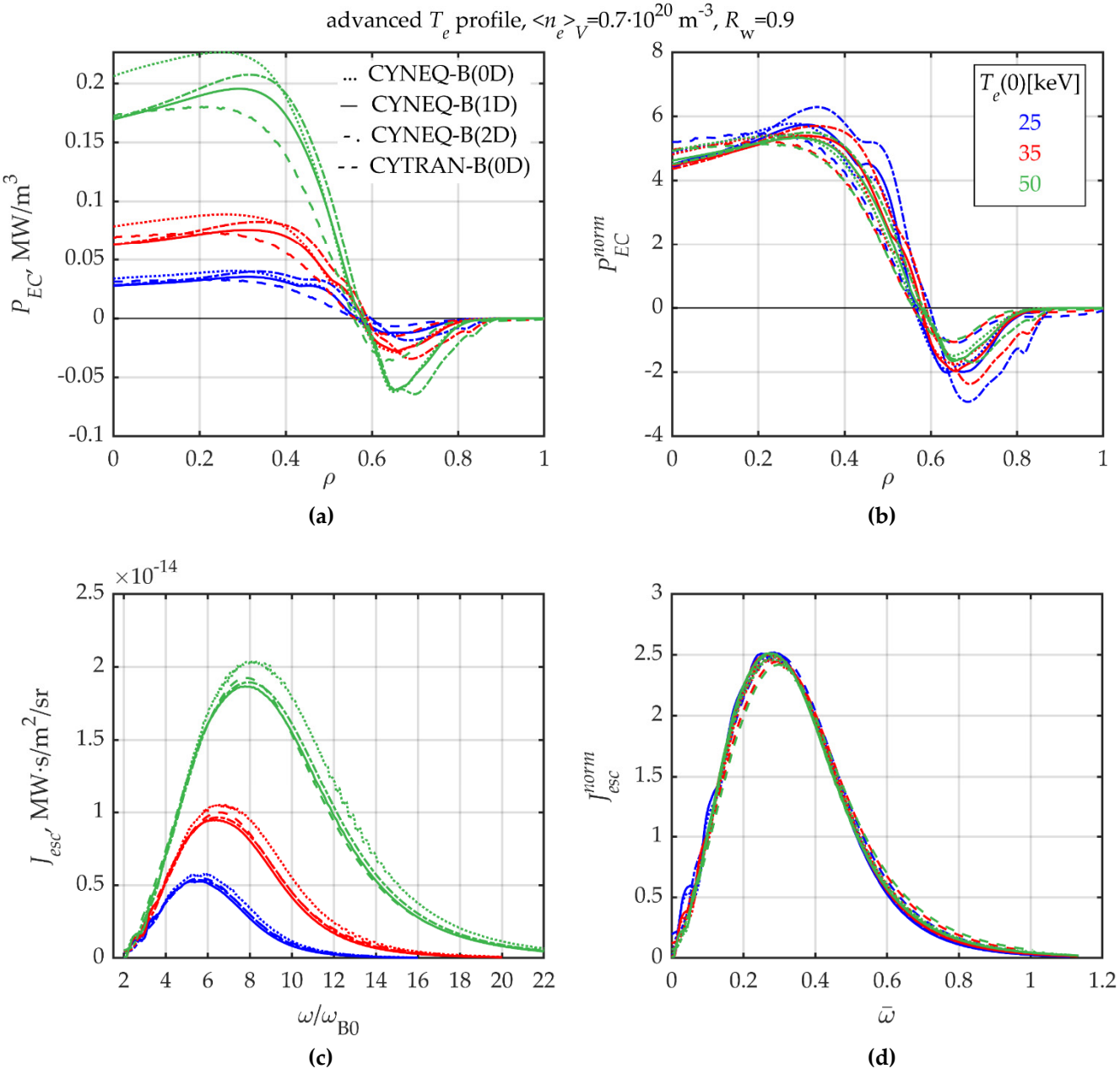

Figure S15. The same as in Figure S12 but for the advanced electron temperature profile and $R_w = 0.9$ (see Table 1 and eq. (27)).

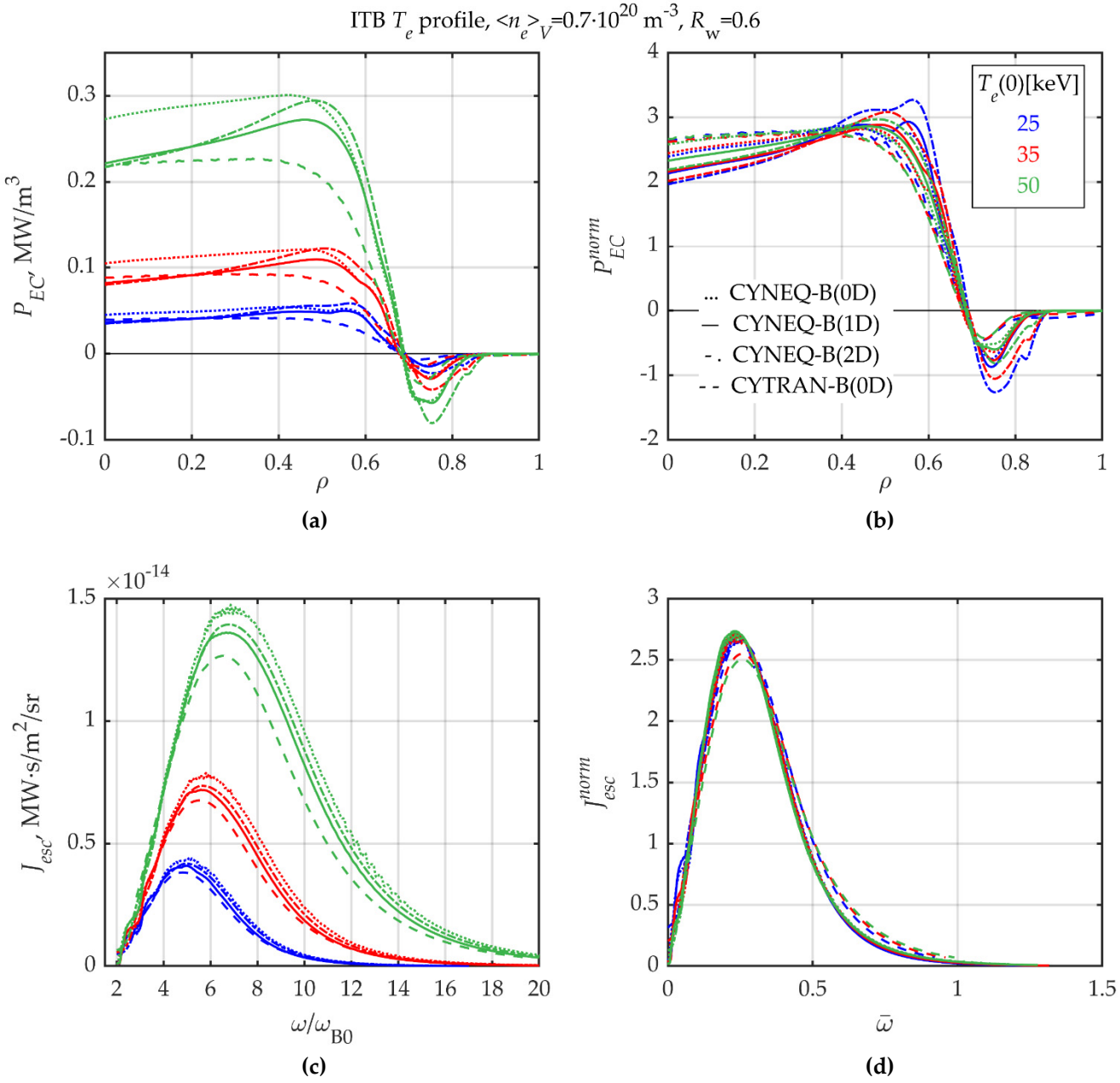

Figure S16. The same as in Figure S12 but for the ITB electron temperature profile (see Table 1 and eq. (27)).

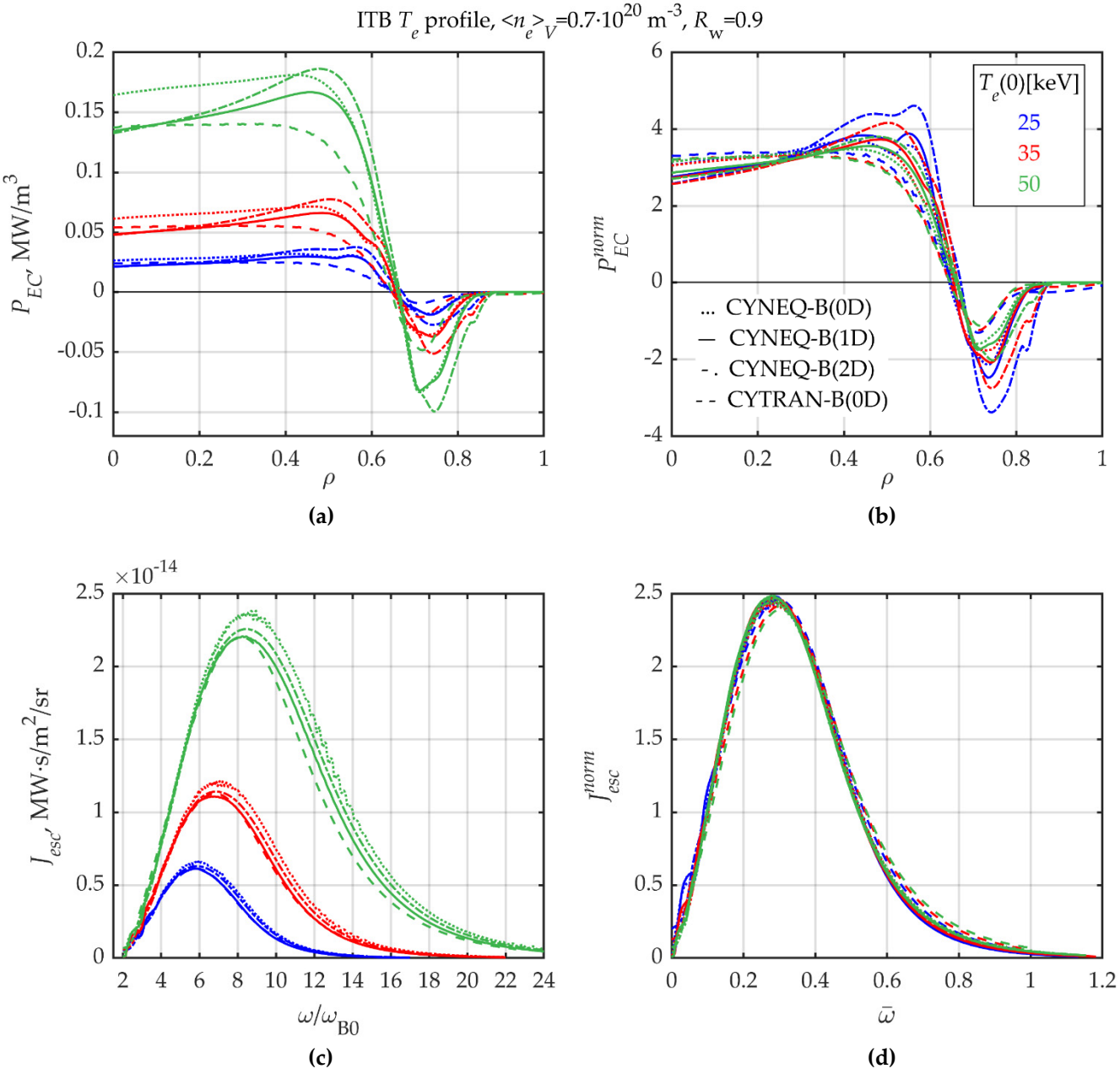

Figure S17. The same as in Figure S12 but for the ITB electron temperature profile and R_w = 0.9 (see Tables 1 and eq. (27)).

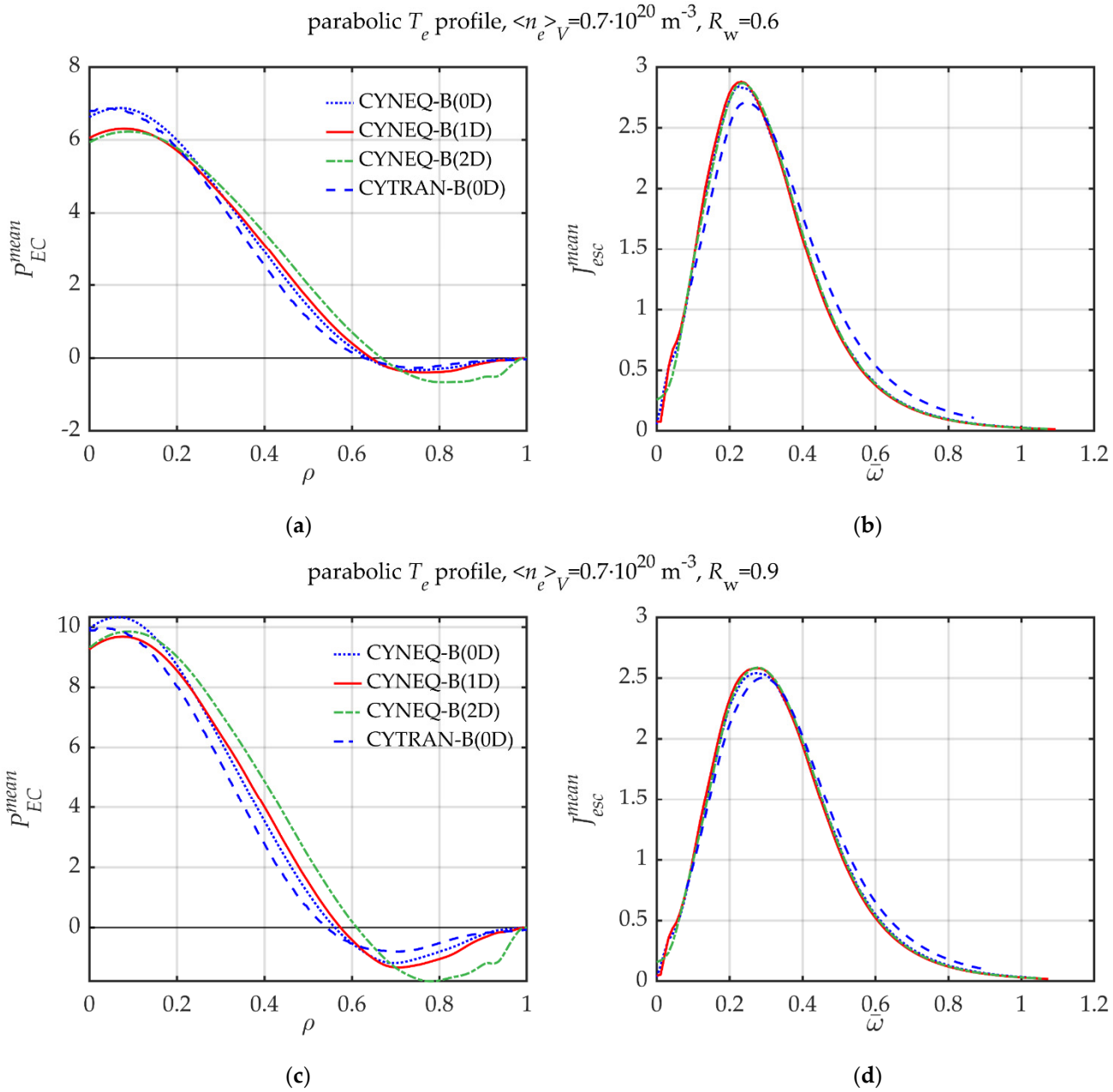

Figure S18. Mean profiles (28) of the normalized radial distribution of the net EC power loss density (**a**), (**c**), and mean spectra (29) of the normalized intensity (**b**), (**d**) for the parabolic temperature profile and non-flat density profile, $R_w = 0.6$ and $R_w = 0.9$ (see Tables 1,2 and eq. (27)).

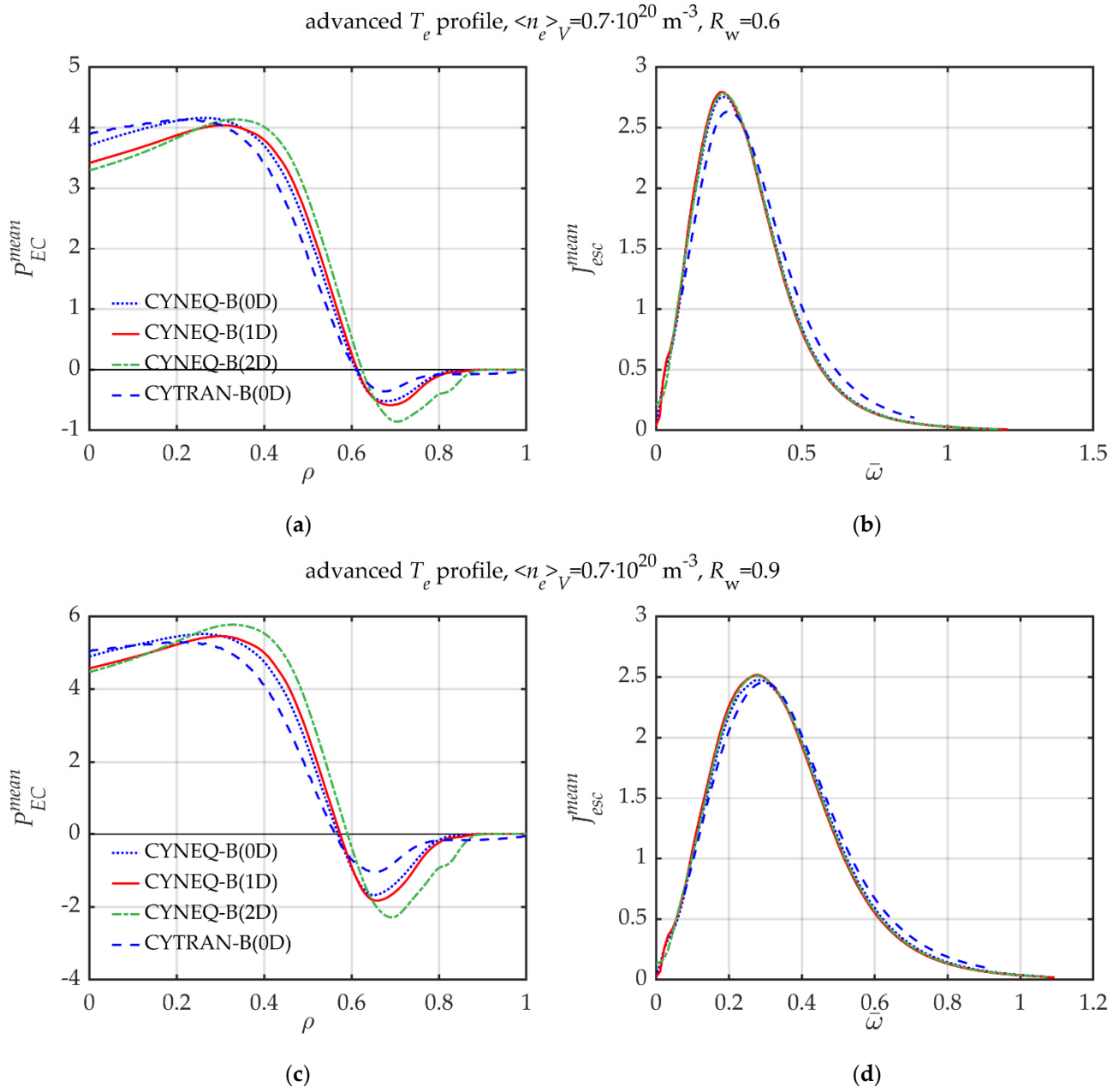

Figure S19. The same as in Figure S18 but for the advanced profile of electron temperature (see Table 1 and eq. (27)).

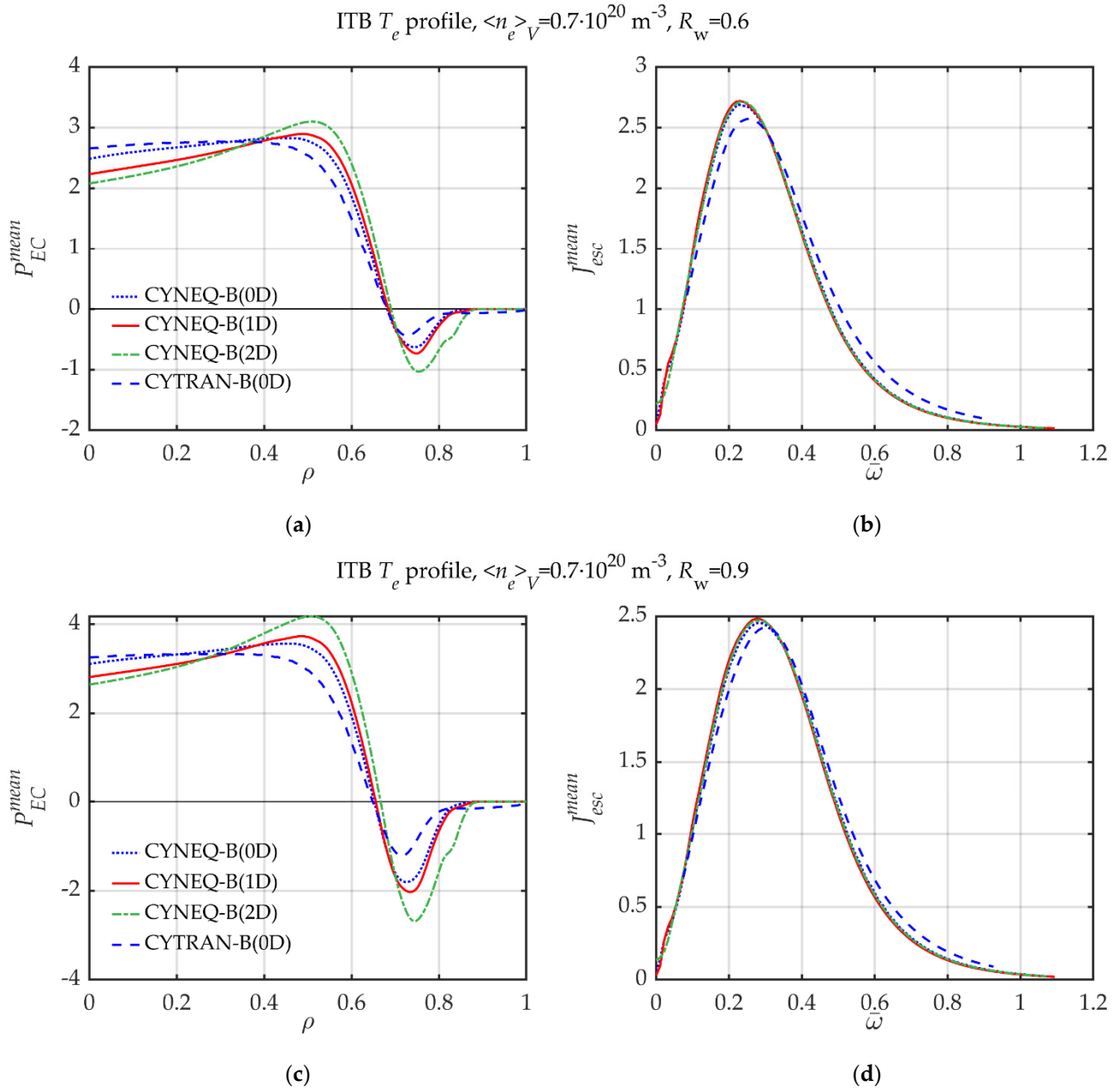

Figure S20. The same as in Figure S18 but for the ITB profile of electron temperature (see Table 1 and eq. (27)).

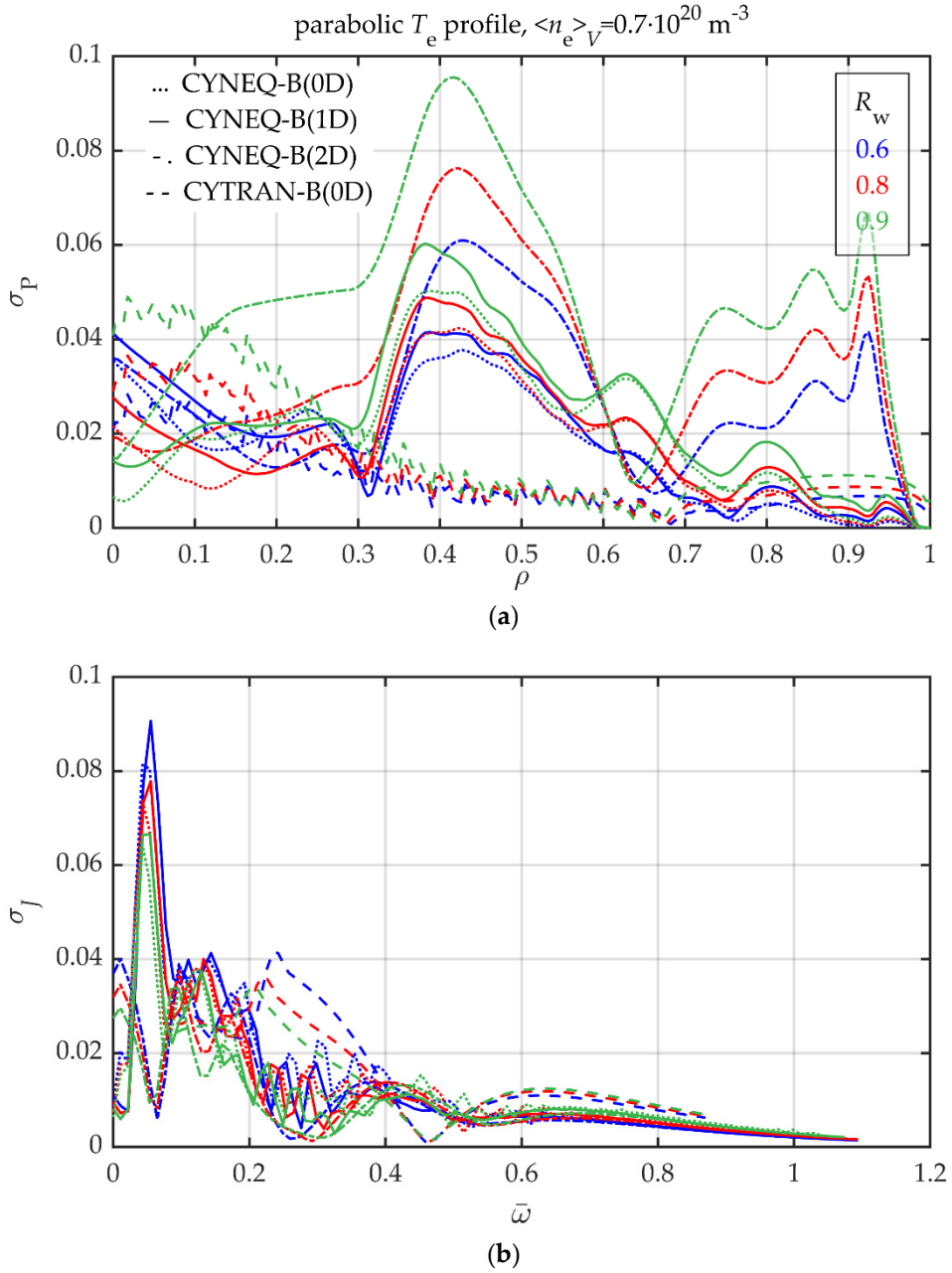

Figure S21. (**a**) Profiles of the relative deviation (30) of the normalized profiles of the EC power loss density from the mean normalized profile (28). (**b**) Profiles of the relative deviation (32) of the normalized spectral intensity of the escaping ECR from mean normalized spectrum (29) for the parabolic profile of T_e, non-flat density profile (see Table 1 and eq. (27)) and different values of R_w. The color of the curve corresponds to the R_w value in the inset.

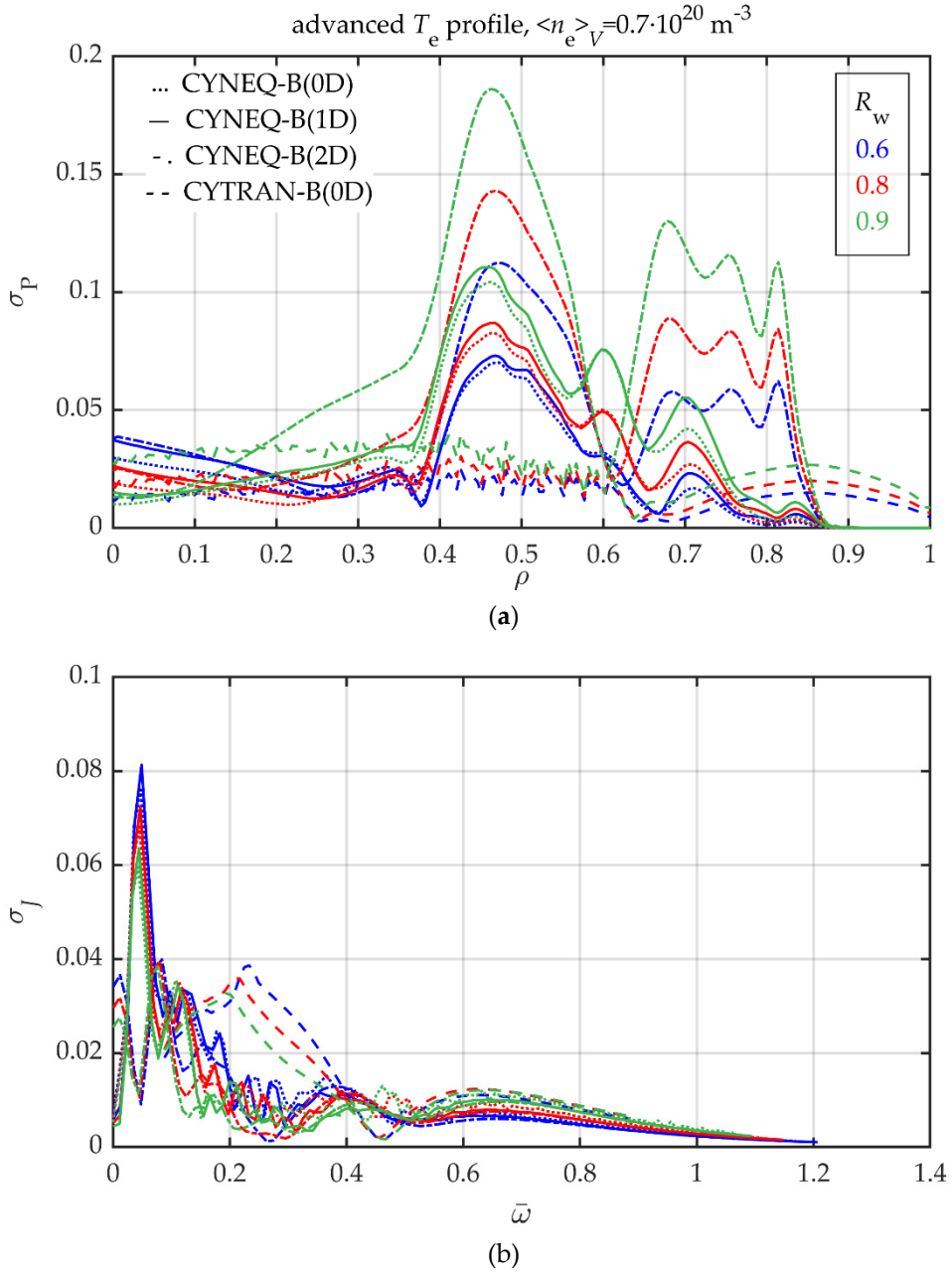

Figure S22. The same as in Figure S21 but for the advanced temperature profile (see Table 1 and eq. (27)).

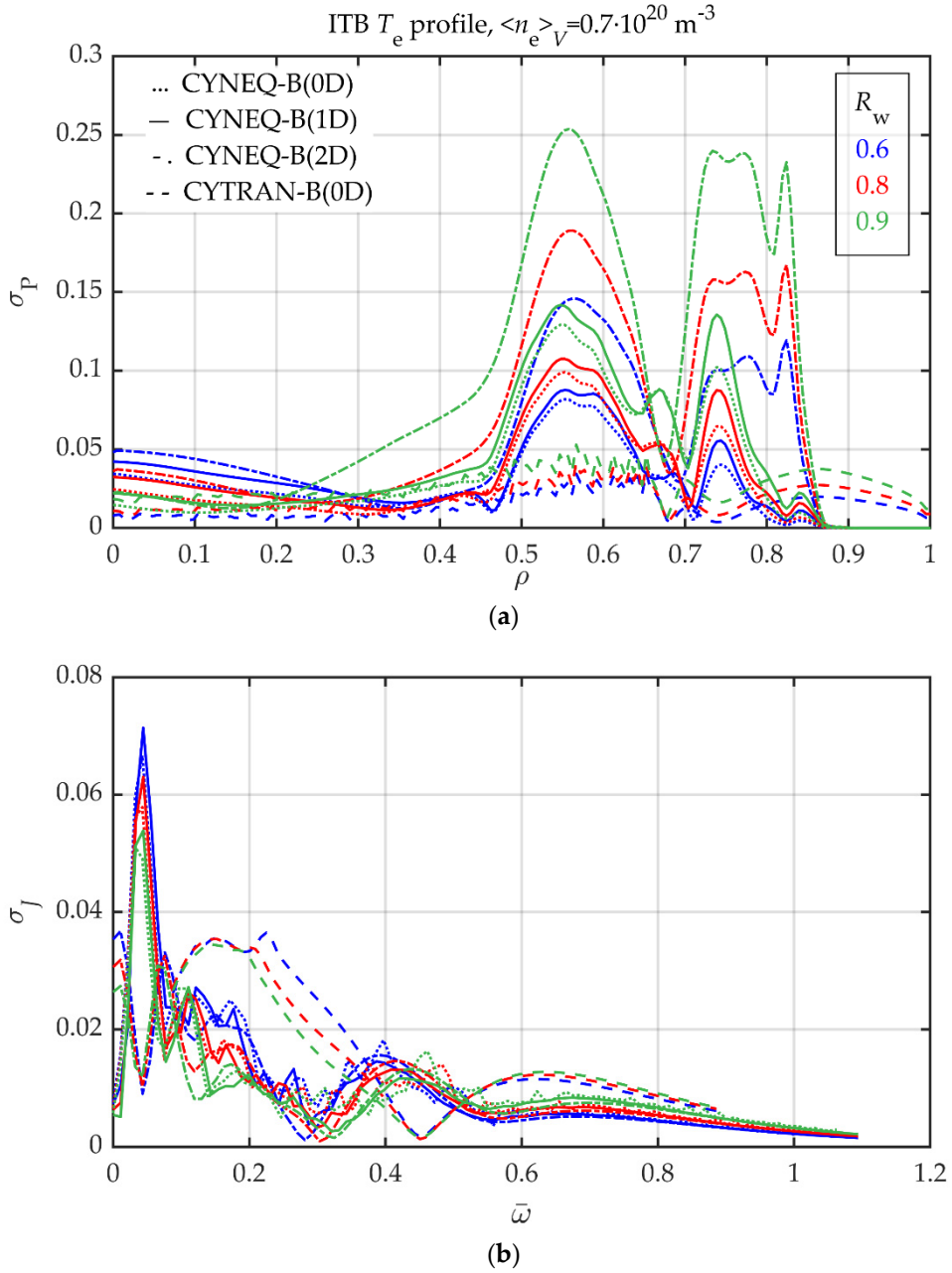

Figure S23. The same as in Figure S21 but for ITB temperature profile (see Table 1 and eq. (27)).

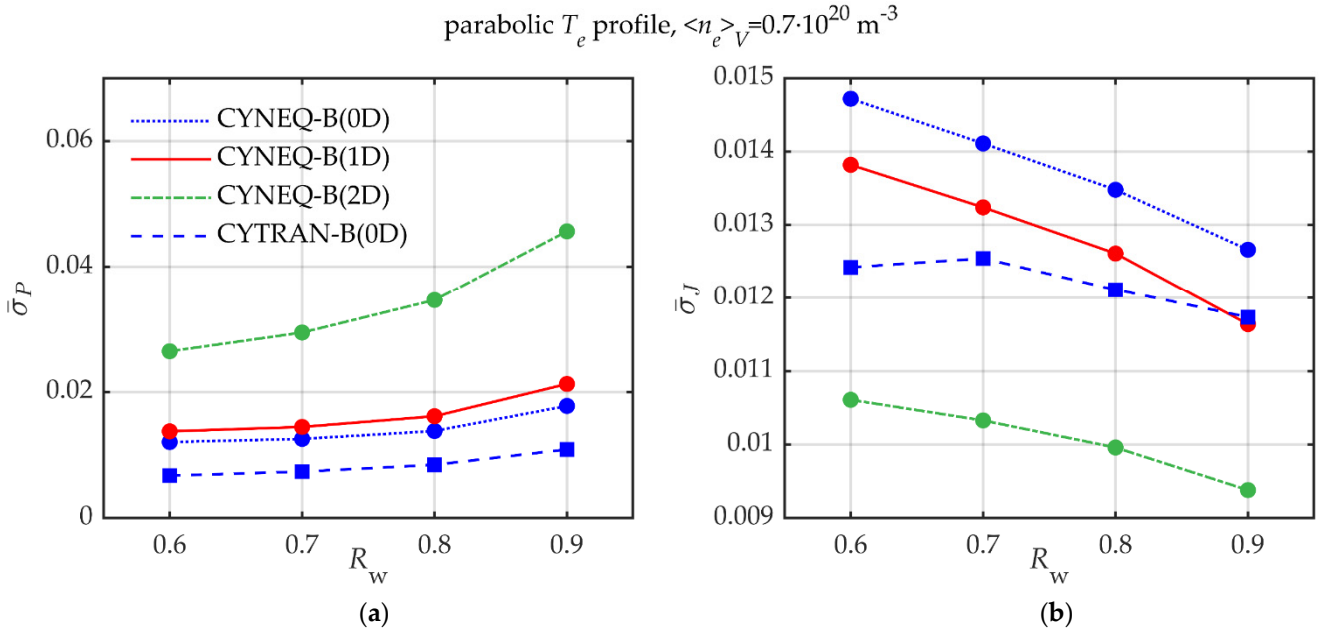

Figure S24. Volume-averaged deviation (31) of the normalized profile of the net EC power loss density from the mean normalized profile (28) (**a**), and spectrum-averaged deviation (33) of the normalized spectra of EC radiation intensity from the mean normalized spectrum (29) (**b**) as a function of the wall reflection coefficient for the parabolic profile of the electron temperature and flat density profile (see Table 1 and (27)).

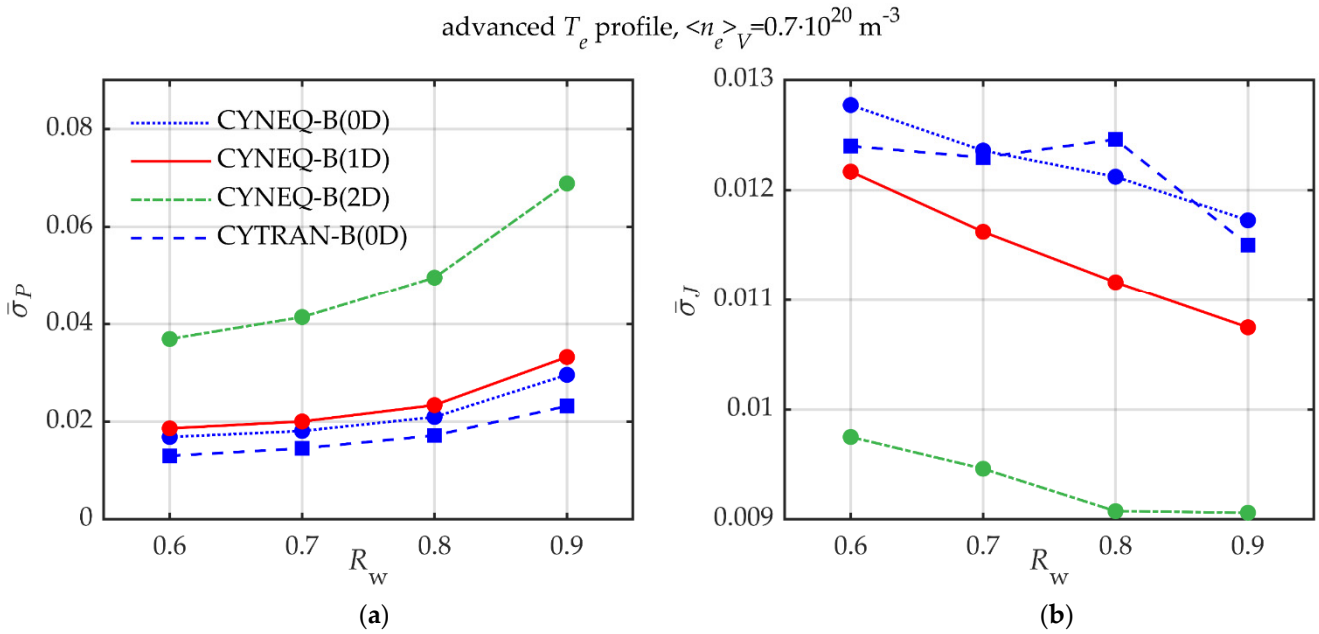

Figure S25. The same as in Figure S24 but for advanced temperature profile (see Table 1 and eq. (27)).

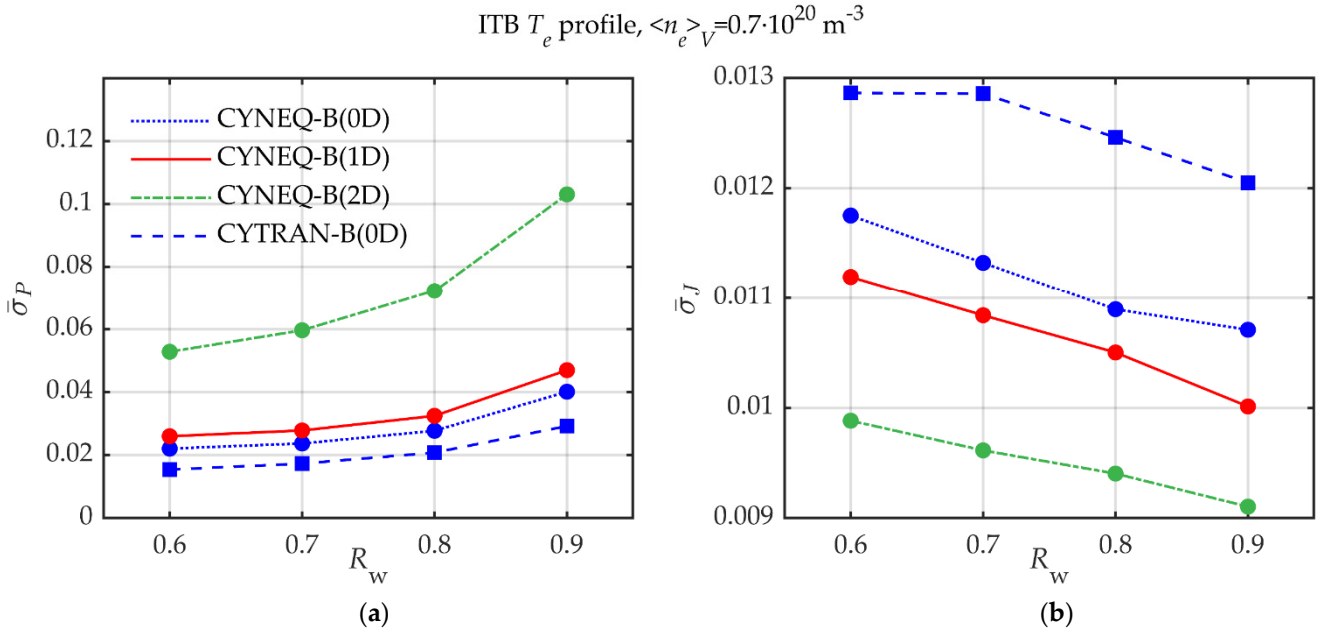

Figure S26. The same as in Figure S24 but for ITB temperature profile (see Table 1 and eq. (27)).

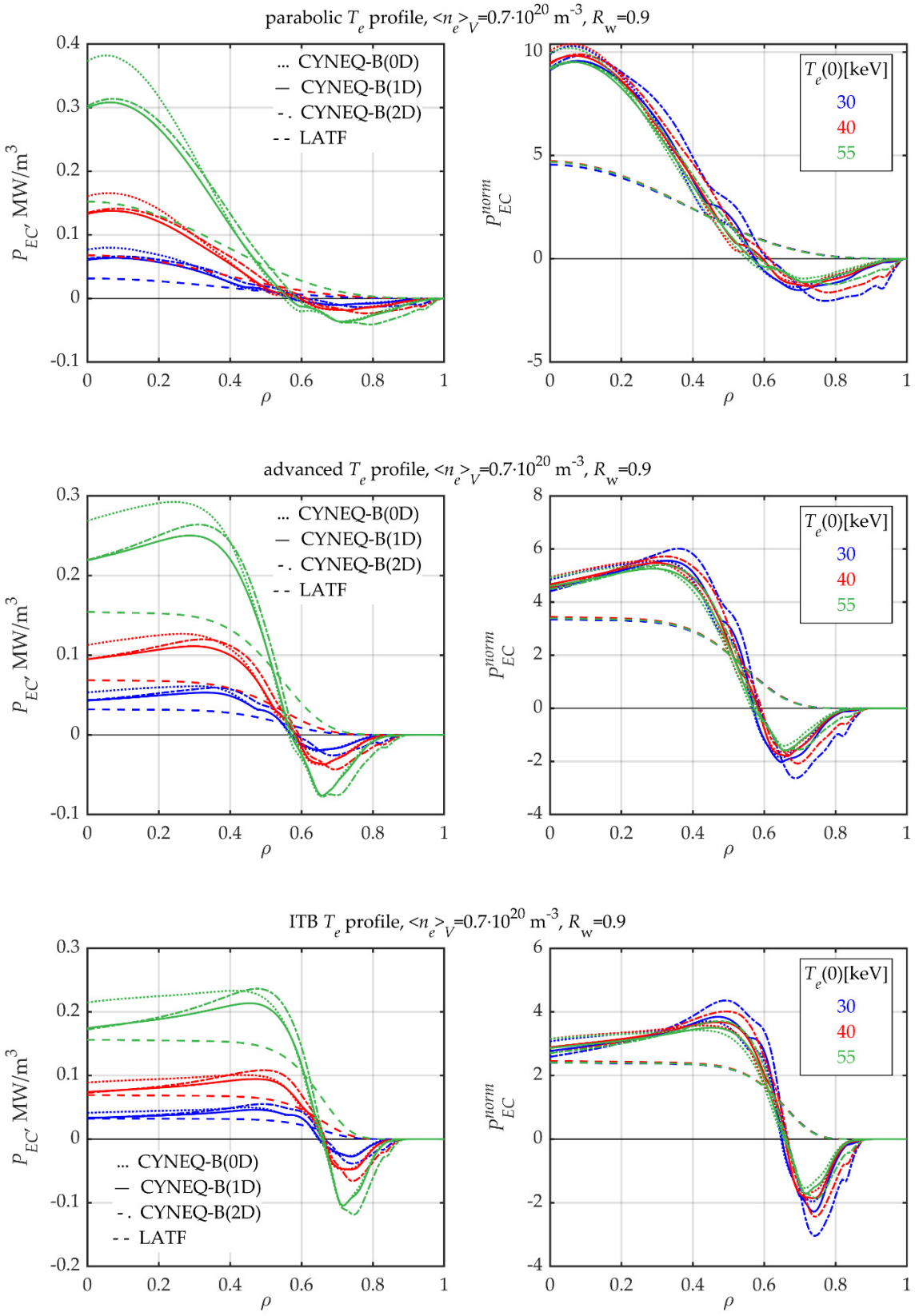

Figure S27. The same as in Figure S12 (a, b) but CYNEQ results are compared with the locally applied Trubnikov formula (LATF) [25] for different T_e profiles and non-flat density profile (see Tables 1,2 and eq. (27)) and R_w=0.9.

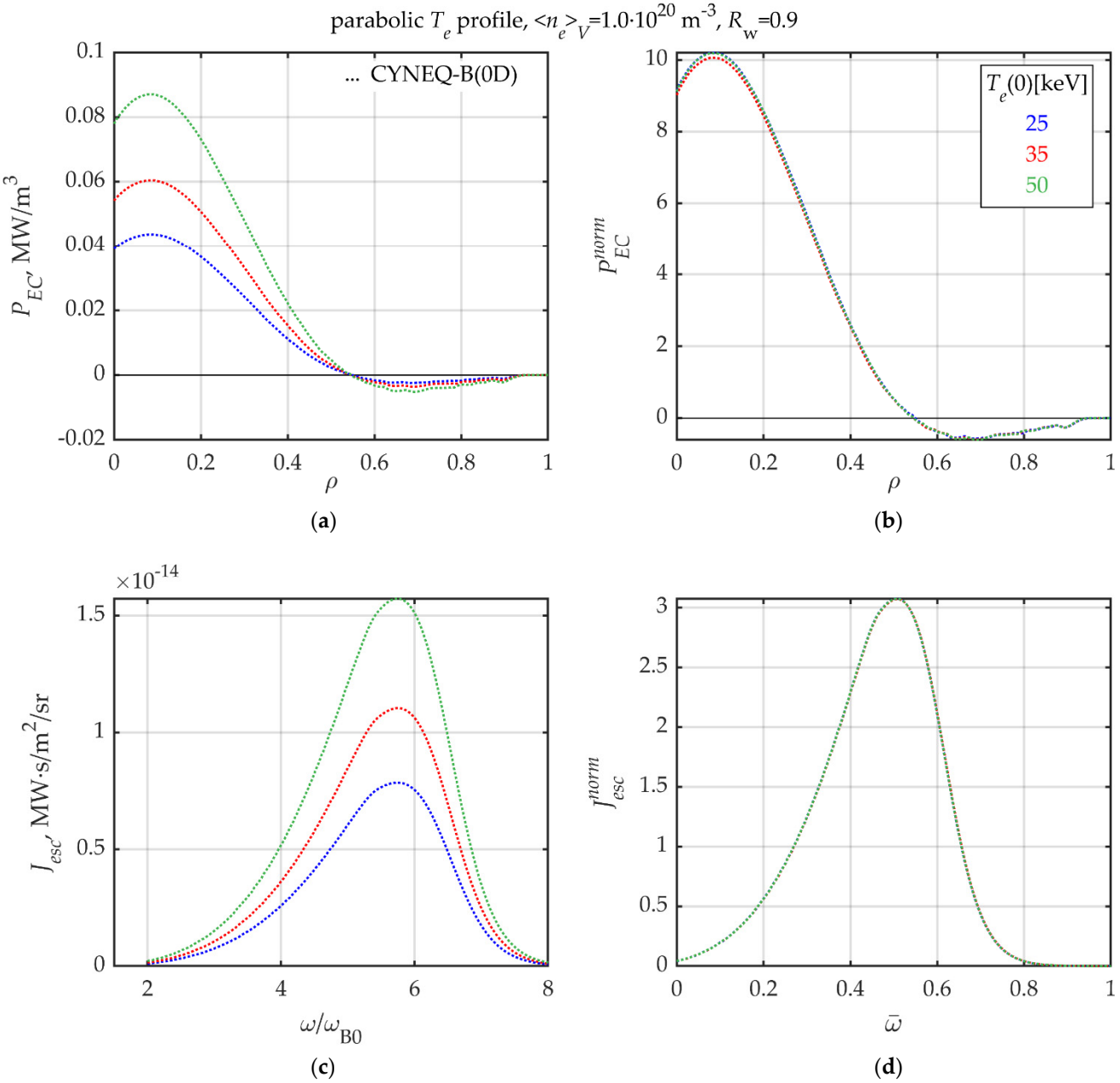

Figure S28. The same as in Figure S12 but for absorption coefficient (36) and R_w = 0.9.

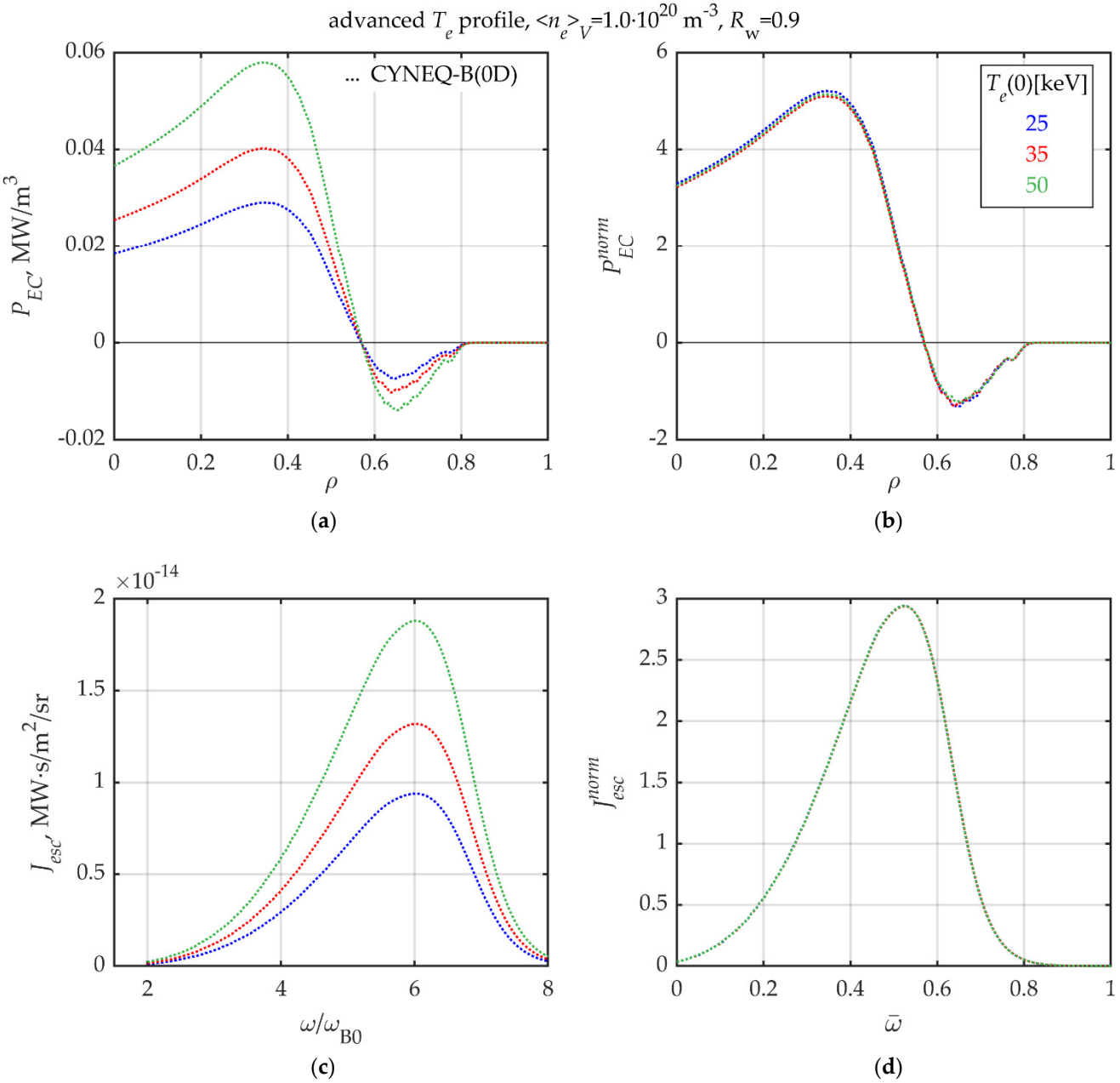

Figure S29. The same as in Figure S12 but for absorption coefficient (36), advanced temperature profile (see Table 1 and (27)), R_w = 0.9.

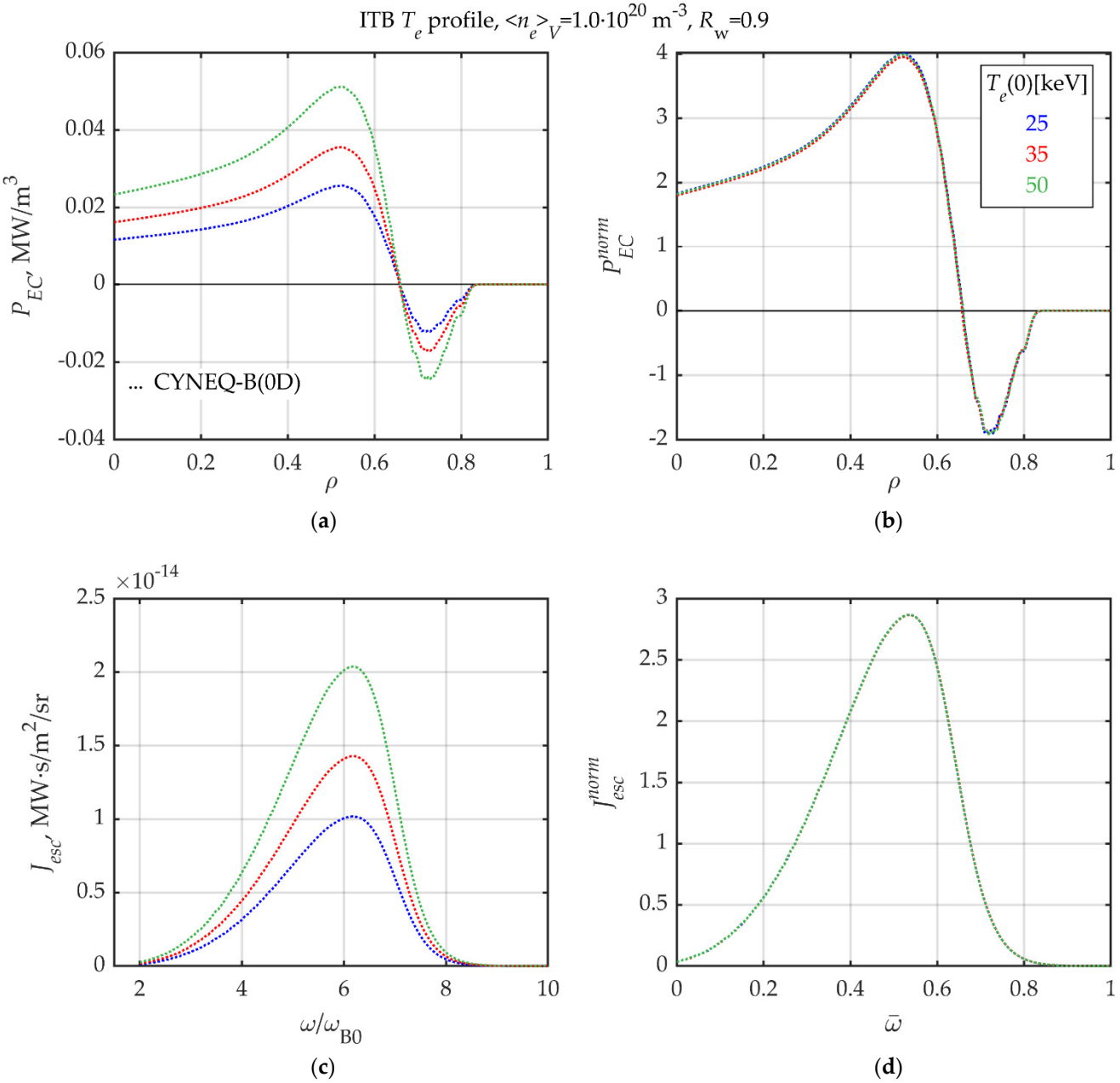

Figure S30. The same as in Figure S12 but for absorption coefficient (36), ITB temperature profile (see Table 1 and (27)), R_w = 0.9.